United States
Department of
Agriculture

Forest Service

Forest
Products
Laboratory

Research
Paper
FPL-RP-499

Structural Performance of Light-Frame Roof Assemblies

II. Conventional Truss Assemblies

Ronald W. Wolfe
Timothy LaBissoniere

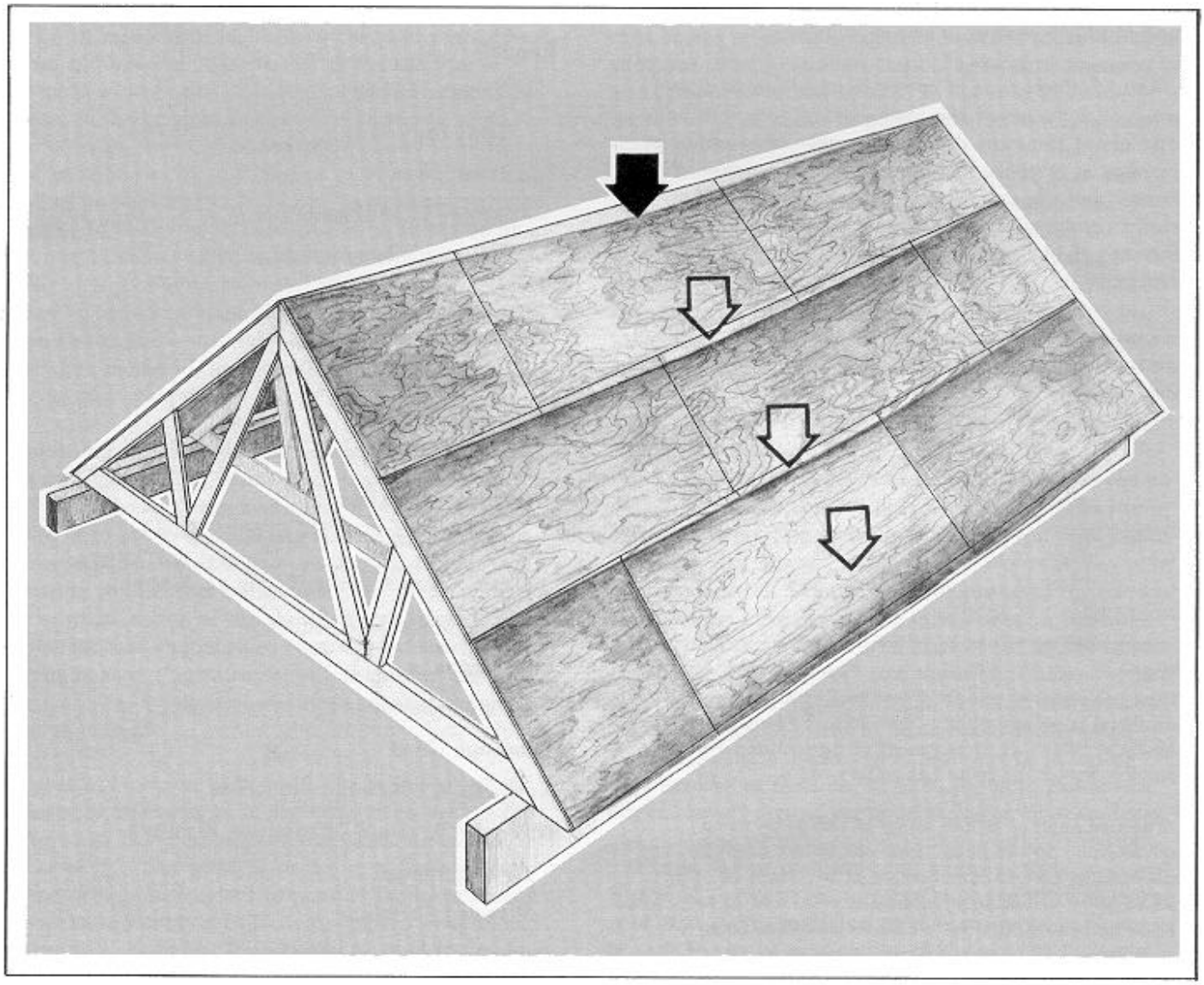

Abstract

This report is the second (Part II) of a three-part series that covers results of a full-scale roof assembly research program. In this study, three trussed roof assemblies were tested to create a database that would aid development and verification of three-dimensional structural roof assembly models. Trusses used in these tests are representative of conventional truss fabrication practice. These roof assembly tests are an extension of a previous study reported in Part I. In that study, the trusses were designed to represent an extreme condition in terms of truss stiffness variation within a single roof and a bias toward failure in wood members rather than in connections.

Results reported in Part II provide information to anyone planning tests of roof assemblies and to those interested in modeling roof assembly performance. Superposition tests are shown to provide a low-risk, accurate method of evaluating assembly response to uniform loads within the elastic range.

Although these tests of conventionally designed roof assemblies displayed less load sharing, they did indicate about the same degree of average truss stiffness increase as a result of composite action between the trusses and the sheathing. For assemblies tested in this study, results support the premise that a load-sharing increase of 15 percent for bending members used in a repetitive member assembly is conservative.

Keywords: Roof assembly, redundant, truss, metal connector plate, vertical load, load distribution, deflection, load capacity

April 1991

Wolfe, Ronald W.; LaBissoniere, Timothy. 1991. Structural performance of light-frame roof assemblies-II. Conventional truss assemblies. Res. Pap. FPL-RP-499. Madison. WI: U.S. Department of Agriculture, Forest Service, Forest Products Laboratory. 32 p.

A limited number of free copies of this publication are available to the public from the Forest Products Laboratory, One Gifford Pinchot Drive, Madison, WI 53705-2398. Laboratory publications are sent to more than 1,000 libraries in the United States and elsewhere.

The Forest Products Laboratory is maintained in cooperation with the University of Wisconsin.

Contents

Page

Introduction 1
Background 1
Objectives and Scope 2
Research Methods 2
  Materials 2
  Individual Truss and Assembly Design 2
  Test Facility 4
    Loading System 6
    Data Acquisition 6
  Test Procedure 7
    Individual Trusses 7
    Roof Assembly Stiffness Tests 8
    Full Assembly Loaded to Failure 8
Results 8
  Individual Trusses 9
    Truss Inspection 9
    Truss Tests 9
  Assembly Load Distribution 11
    Individual Truss Load 11
    Assembly Loads 11
    Assembly Strength 11
Analysis of Results 15
  Truss Stiffness 15
  Assembly Effects 15
    Composite Action 17
    Load Sharing 17
  Distribution of Loads Within an Assembly. . . . 19
  Failure Modes and Sequence 20
Conclusions 20
Acknowledgments 21
Literature Cited 21
Appendix A-Material Properties 22
Appendix B-Load-Distributing Elements 24
  Bearing Plates 24
  Plywood Sheathing 25
Appendix C-Connections 27
Appendix D-Load-Sharing Evaluation 32

Structural Performance of Light-Frame Roof Assemblies II. Conventional Truss Assemblies

Ronald W. Wolfe, Research General Engineer
Timothy LaBissoniere. General Engineer

Forest Products Laboratory, Madison, Wisconsin

Introduction

The design methodology used for conventional light-frame roof assemblies has evolved over 150 years, blending art and science. Prior to the 1950s, the master craftworkers made most decisions about form and function on the basis of experience. This process, while slow to accept innovation, provided a history of reliable performance. In the 1950s, scientific developments in adhesives and mechanical connections began to have a significant effect on the design and construction of light-frame roof assesmblies in the form of exterior grade panel products and metal plate connected wood trusses. However, market demands limited their application to repetitive member assemblies that were similar to the dimension lumber rafter and board sheathing systems they replaced.

Trussed roof assembly design methodology has changed little over the past 30 years. Each truss is designed to carry full tributary area load. The 15-percent load-sharing increase to the bending stress for repetitive member use has less influence on the allowable load on a truss than it does on a lumber rafter. Benefits of diaphragm action of the sheathing are treated as inherent and unquantified regardless of the type of framing used. Light-frame roof assemblies are still treated as a collection of independent structural elements.

To provide a method to quantify the beneficial effects of assembly interactions, analytical models are needed to show how assembly interactions affect assembly load capacity. This study is part of a roof assembly research program designed to provide the tools needed to evaluate assembly sensitivity to various design and construction variables. Results will be used to develop and evaluate three-dimensional structural roof assembly models.

Background

This report is the second (Part II) of a three-part series that covers results of a full-scale roof assembly research program. Part I reported tests of individual trusses and full-scale roof assemblies. In these tests, trusses were fabricated using 16-gauge steel metal connector plates (MCPs) placed at critical locations where 20-gauge would normally be used and lumber that had been sorted into three distinct stiffness categories. The purpose of that study was to force failure to occur predominately in the wood members and to provide a slightly exaggerated representation of how relative truss stiffness affects load distribution within an assembly. The third report (Part III) will evaluate the performance of rafter roof assemblies.

The Part I report (Wolfe and McCarthy 1989) provides a survey of available literature on the structural performance of light-frame roof assembly and looks at the potential advantages of assembly interactions. The literature review indicates that data on the structural performance of roof assemblies are limited from the viewpoint of those interested in model development. Previous assembly tests have given little quantitative information on the load-sharing characteristics of redundant assemblies. The roof assembly tests described in the Part I report, although representing an extreme case for truss stiffness variability, indicate that load sharing could benefit the most limber truss, reducing its tributary area load by as much as 30 to 40 percent. The actual benefit would depend on the correlation between truss stiffness and strength and assembly load distribution patterns. Based on observations from limited tests and historical performance of light-frame repetitive member roof assemblies, analytical models supporting the acknowledgment of assembly performance could have a significant impact on reducing the cost/benefit ratio for these assemblies.

Objectives and Scope

The roof assembly tests described in this report (Part II) were conducted to provide a basis for the development and verification of three-dimensional structural roof assembly models. Tests were conducted on individual trusses and full-scale roof assemblies. Results were evaluated to assess assembly interaction effects of individual truss stiffness and strength.

Truss configurations selected were two Fink and one scissors (Fig. 1). The two Fink configurations were selected to provide some direct comparisons with the tests reported in Part I. The scissors configuration was selected to evaluate the ability of models to accurately represent the importance of horizontal restraint at the truss reactions.

Research Methods

Tests to evaluate roof assembly performance included tests of material properties, truss stiffness and strength, and full assembly load response. Material property tests included bending stiffness of the lumber and plywood sheathing and moisture content and specific gravity of the lumber. Lateral nail tests were also conducted to evaluate the plywood sheathing to truss connection and the performance of the MCPs. Tests included measurement of the load-deflection response outside and inside the assembly and the load capacity of individual trusses tested outside the assembly. A series of full assembly tests under vertically applied loads were conducted in a three-dimensional test frame. All vertical reactions, some horizontal reactions, vertical deflections, joint deformations, sheathing-chord slip, and horizontal displacements at the reactions were measured and recorded by a computer.

The effects of assembly interactions were evaluated by comparing the truss performance under the boundary conditions imposed by the constructed full assembly to those measured when the trusses were tested individually. The small number of individual trusses tested made it unfeasible to directly evaluate full assembly effects on truss load capacity in this manner. However, by comparing load capacity of trusses tested in the full assembly to those tested outside and by noting how loads are distributed in the full assembly, it is possible to assess how an individual truss can affect the load capacity of the full assembly.

Materials

Raw materials for this study included lumber, MCPs, plywood sheathing, nails, and metal wind clips. Two hundred twenty-eight pieces of 2 by 4 No. 2 Dense Southern Pine lumber were purchased from a local retailer. Although all the lumber was not grade stamped, it did appear to meet all the visual requirements of the grade. The MCPs, provided by the truss fabricator, were 20-gauge (0.36-in.-thick) galvanized steel with a tooth length of 5/16 in. and a tooth density of 9.1/in^2. Forty-two 4- by 8-ft sheets of 15/32-in. three-ply Southern Pine plywood were supplied by industry cooperators, along with individual sheet stiffness values determined according to ASTM D 3043 Method C (ASTM 1981b). Plywood sheets, graded CD exposure 1, had an average bending stiffness of 1.8×10^5 lbf in^2/ft, with a coefficient of variation (COV) of 12 percent. Nails 2 in. long with a 0.113-in. diameter were used to fasten the sheathing to the trusses and were classified 6d common. The wind clips used to hold the trusses in place on the bearing plate were 20-gauge galvanized steel, such as those commonly found in commercial light-frame construction.

Prior to truss fabrication, each piece of lumber was marked with an identification (ID). Its modulus of elasticity (MOE) was also determined using an E-computer, an analytical device that determines MOE as a function of the natural frequency of vibration. Every tenth piece of lumber was also tested using a center-point load on a simple span as a static check on the vibration value.

Individual Truss and Assembly Design

Truss configurations used in this study were two Fink, one with a top-chord pitch of 6:12 and one with 3:12, and one scissors (Fig. 1). Differences between the Fink configurations in this study and those in the Part I report (Wolfe and McCarthy 1989) were the lumber, connections, and the lack of a top-chord splice. In Part I, (1) the lumber was selected to represent a wide MOE range for No. 2 Southern Pine, (2) 16-gauge MCPs were used on critical joints to counteract the bias in favor of short-term-test steel failure, and (3) a splice joint in the top-chord panel adjacent to the peak played a major role in the failure of the 6:12 roof assembly.

All trusses were designed with a span of 28 ft and a spacing of 2 ft on center, using No. 2 Dense Southern Pine lumber. In each case, the Truss Plate Institute (TPI) design specification was used to derive a design load given the lumber and truss configuration (TPI 1985). The normal residential roof is designed for a bottom-chord dead load of 10 lb/ft^2 for the 3:12 Fink

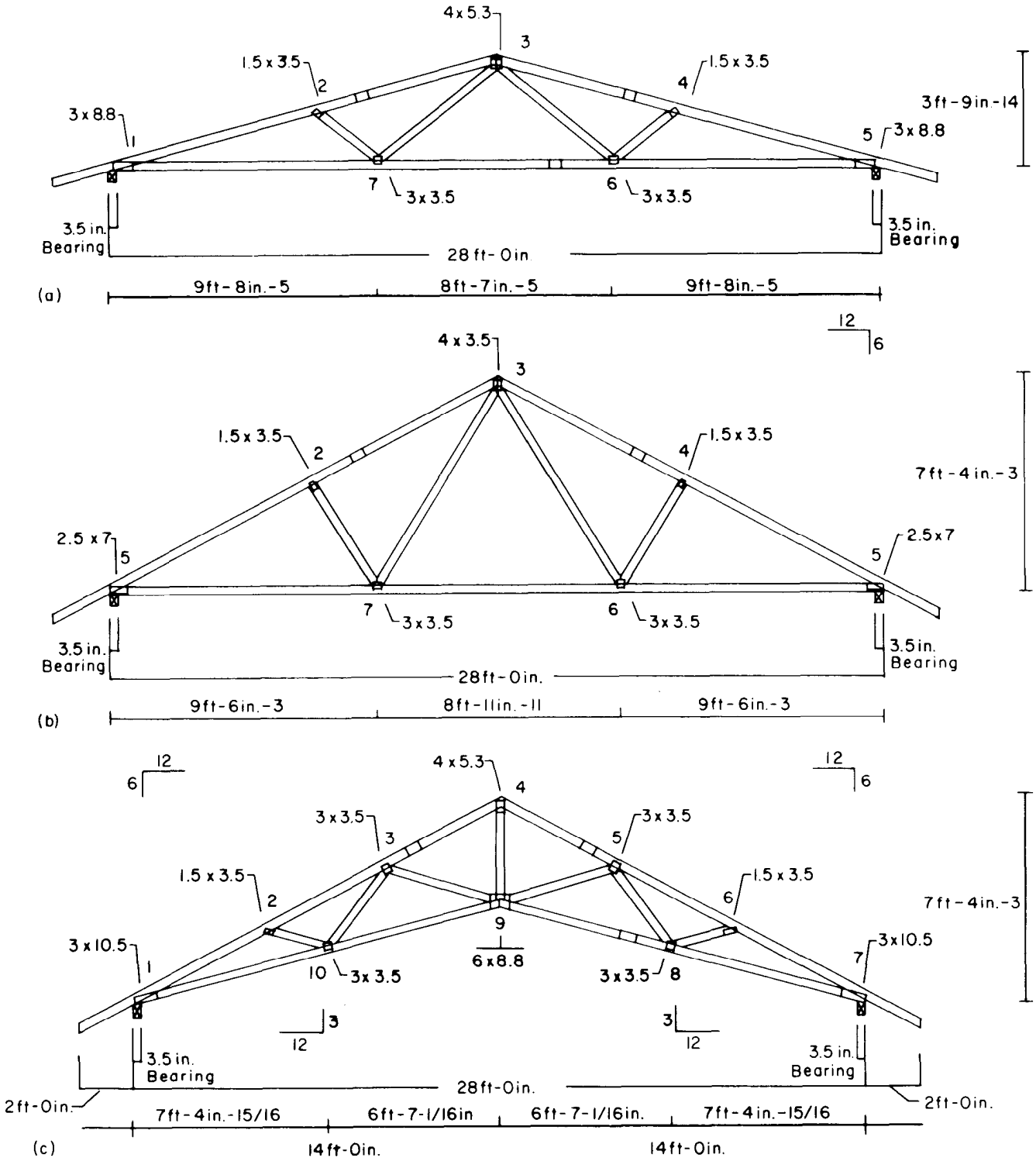

Figure 1—Three truss configurations tested in this study: (a) 3:12 Fink; (b) 6:12 Fink; (c) 6/3:12 scissors. All trusses designed to span 28 ft using No. 2 Dense Southern Pine and 20-gauge metal connector plates. (ML90 5404)

configuration and 8 lb/ft^2 for the 6:12 Fink and scissors configurations. Our tests were designed for load to be applied only to the top chord with an equipment dead load of about 7 lb/ft^2. We asked the fabricator to reevaluate the truss design loads with dead loads of 7 lb/ft^2 on the top chord and 1 lb/ft^2 on the bottom chord. Thus, the design loads for this case were 31, 38, and 38 lb/ft^2 for the 3:12, 6:12, and scissors configurations, respectively. In each case, the most highly stressed members were in the top chord adjacent to the heel connection. For the 31-lb/ft^2 design load, stress on these members ranged from 0.8 to 0.9 times the allowable stress. Stress was evaluated on the basis of the combined stress index (CSI) described in the National Design Specification (NFPA 1988). For the 38-lb/ft^2 design loads, the CSI values ranged from 0.76 (6:12 Fink) to 0.78 (3:12 Fink and scissors).

Assuming a linear relationship between load and CSI and that truss capacity is controlled by wood member strength rather than connector strength, we modified the manufacturer's designated design load by extrapolating to a CSI of 1.0. This permitted direct comparison of truss performance in this study with that given in the Part I report (Wolfe and McCarthy 1989). Thus, throughout this report, DSN is used to refer to the top-chord load at critical CSI of 1.0 and indicates loads of 80 lb/lin ft (3:12), 100 lb/in ft (6:12), and 98 lb/lin ft (scissors).

Each roof assembly included eight trusses, 15/32-in. plywood sheathing, and a gable end. For each roof assembly, 12 trusses were individually tested in the order they were taken off the pile as shipped from the truss plant. Four of the 12 trusses were tested to failure; the remaining 8 were tested for stiffness only and were then fastened using 20-gauge wind clips at 24-in. intervals along the bearing plate (Fig. 2). Trusses were held in position using 2 by 4 cross bracing while the sheathing was nailed in place. For each roof assembly, sheathing was applied so that full sheets were adjacent to the peak and partial sheets were fastened to the eaves. Sheathing patterns and the corresponding measured bending stiffness of each sheet are given in Appendix A. The gable end for each roof was made using one of the failed trusses sheathed with plywood. The gable end used for the 6:12 Fink roof was also used for the scissors roof.

For the three roof assemblies, only once did the relative stiffness of a truss influence its location in the assembly. Concern for possible lateral deformation of the scissors assembly prompted us to use the stiffest scissors truss on the open end of the roof. The order in which individual trusses were placed in their respective assemblies is given in Appendix B.

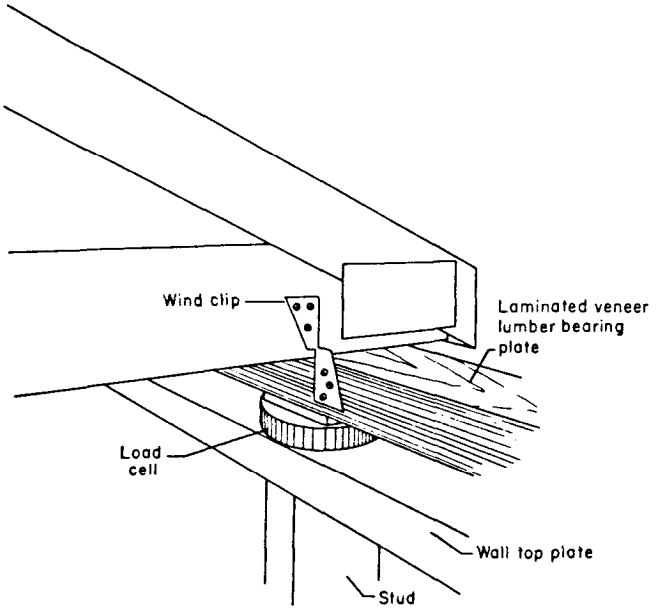

Figure 2—Truss reaction detail showing metal wind clip used to fasten the truss to the LVL bearing plate. (ML89 5592)

Two sheathing nailing patterns were used to permit some evaluation of nailing influence on assembly performance. The assemblies were first tested with 6d common nails spaced 12 in. on center. Additional nails were then added to reduce this spacing to 6 in. for a final series of stiffness tests and the test to failure. The 6:12 Fink assembly had the nails spaced 6 in. on center only at the edges of the plywood sheets during its second set of stiffness tests and the test to failure.

Test Facility

A three-dimensional structural test facility (Fig. 3) (Boller 1972) was used for this study. The roof assembly test setup described in Part I (Wolfe and McCarthy 1989) was modified slightly to accurately characterize individual truss as well as full assembly performance. Modifications were an improved individual truss-bracing system, a stiffened reaction support wall, an addition of a gable end for each roof assembly, and added data acquisition equipment to measure assembly horizontal reactions and connection displacements.

For the individual truss tests, a new bracing method (Fig. 4) was used to minimize interference between the bracing and truss vertical deflection. Rather than applying lateral restraint directly to the truss chord, a plywood-stiffening element was fabricated to restrain chord deformation in the horizontal plane. The vertical loading rods were then held in place by running them through vertical sleeves fastened to the test frame. Restraint on the loading rods was transferred to the

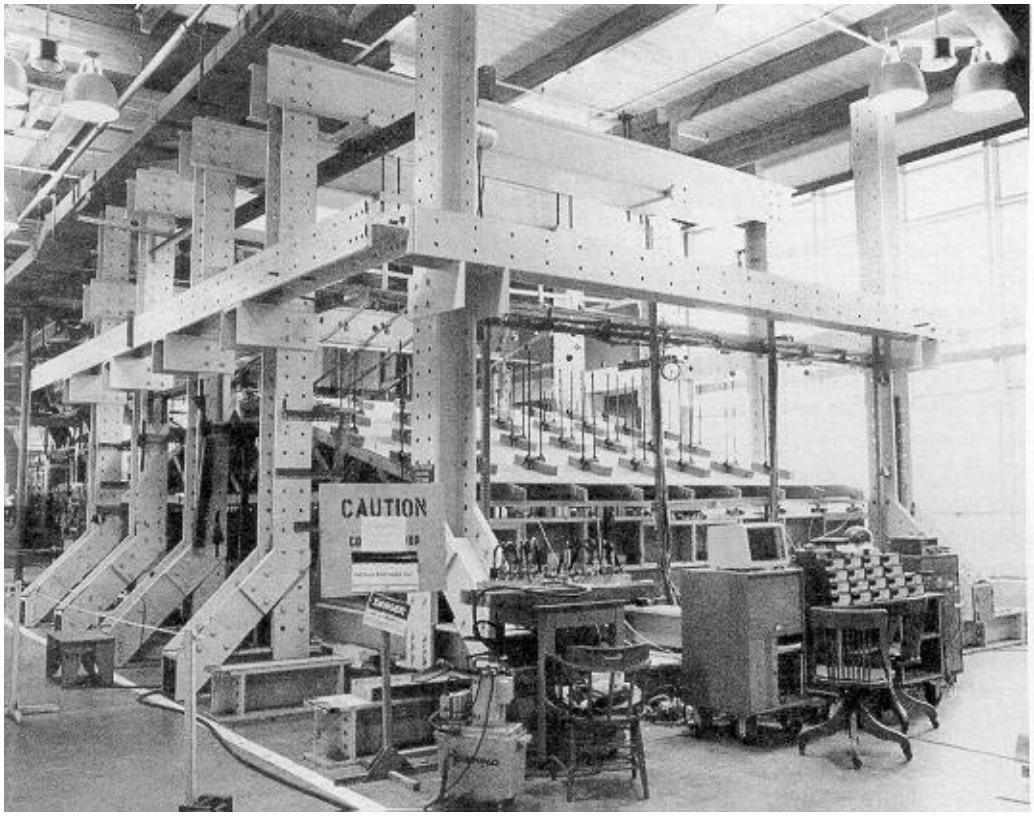

Figure 3—Three-dimensional structural test facility containing a test roof assembly. (M87 00240-4)

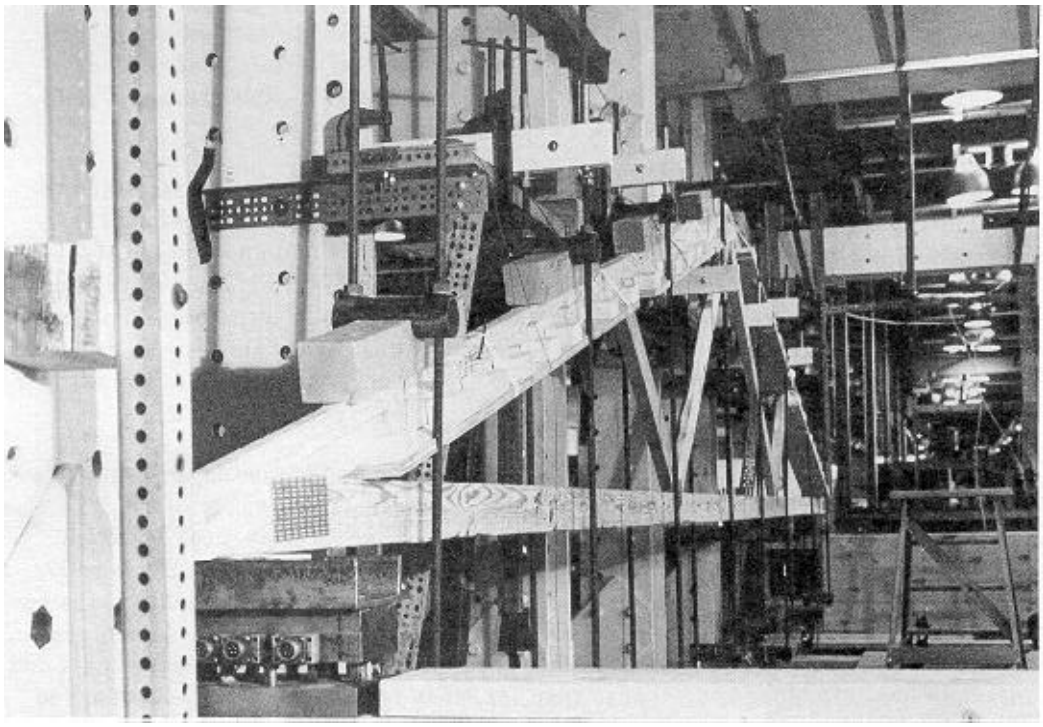

Figure 4—Individual truss test bracing. Plywood board with attached 2 by 4 blocking was used to confine the truss chord in a single plane, while the loading rods were held in alignment by passing through a sleeved &ace attached to the test frame. (M86 0237-5).

top chord of the truss through the loading blocks, which had 16d nail points protruding 0.25 in. into the top edge of the chord. By increasing the effective out-of-plane stiffness of the chord and placing lateral restraints at 41-in. intervals along the chord, the Euler buckling load was conservatively estimated to be more than 10,000 lb.

Reaction support walls were designed to evaluate the effects of lateral restraint on roof stiffness. The trusses were attached to bearing plates that were supported vertically on load cells at each truss reaction location. Nineteen-foot-long pieces of laminated veneer lumber, cut to size and tested to determine MOE, were used for bearing plates. Bearing plate sections were 2 by 3 in. for the two Fink configurations and 2 by 4 in. for the scissors configuration. In the horizontal plane, the bearing plates (Fig. 3) were designed as pinned-end beams with an 18-ft span. The middle truss reaction load cells were capable of measuring both vertical and horizontal reaction forces; therefore, some tests were conducted with a horizontal reaction at midspan of the bearing plate.

A steel C channel attached to the top of the load cell at the middle truss reactions gave us the option of allowing the bearing plate to move freely in the horizontal plane or to be restrained. A wedge block placed between the bearing plate and the side of the C channel caused horizontal thrust reaction forces on the bearing plate to be transferred into the load cell.

Loading System

The loading mechanism and load-point locations over the truss span were the same as those described in Part I (Wolfe and McCarthy 1989). In summary, loads were applied at eight locations along the top chord of each truss through 20-in.-long load distribution blocks. Four loading rams with a 10-in. stroke and a 10,000-lb capacity were used for each truss. The ram control manifold contained a control valve for every two rams, permitting roof load to be applied to half a truss span at a time.

Data Acquisition

The data acquisition system was expanded from that described in the Part I report (Wolfe and McCarthy 1989) to include additional information on assembly interaction effects on truss stiffness and strength. For the individual truss tests, we included horizontal thrust measurements and joint deformations, adding 5 channels to the individual truss data files. For the roof assembly tests, the expansion added 31 channels. Seven of these channels measured the peak deflections on the interior trusses, four channels measured the sheathing-chord slip displacements, and 10 channels measured joint displacements on two trusses. Four reaction channels were added to measure horizontal thrust: two at the reactions of the fifth truss and two on cables to measure bearing plate separation force. The support wall horizontal displacements, measured using dial gauges as reported in Part I, were measured using six potentiometers in this study.

Vertical deflections were measured using rotary linear resistance potentiometers (RLRPs) (resolution of ±0.002 in.) attached to an overhead yoke. Lines used to drive the potentiometer pulleys referenced points along the centroidal axis of the top chord over the reactions, the top-chord node points, the peak, and at the middle of two top-chord panels-adjacent to peak on north slope and adjacent to heel on south slope. For the full assembly tests, 0.5-in.-diameter holes were drilled through the sheathing at these referenced points to permit access to the top chord.

Load cells measured vertical reactions and horizontal thrust. For the individual Fink truss tests, a 10,000-lb capacity uniaxial load cell measured the north vertical reaction, and a triaxial load cell (5,000-lb capacity vertical, 2,000-lb capacity horizontal) measured the south end, measuring both vertical and horizontal reactions. Horizontal and vertical forces were measured at both reaction points of the scissors trusses. For the assembly tests, the triaxial load cells were used only for the fifth truss; however, cables attached to the wall bearing plates, in series with 1,000-lb capacity load cells, also measured wall separation forces resulting from horizontal thrust. Other truss reactions in each assembly were supported on uniaxial load cells. In addition to end reactions, each gable end had a third reaction support at midspan.

Sheathing-chord slip displacements were measured using linear variable differential transducers (LVDTs) with a 0.1-in. working range and an accuracy of ± 0.1 percent. The LVDTs were attached to the truss top chord and reacted against a metal angle attached to the sheathing. A total of 16 channels were dedicated to sheathing-chord slip measurement, four channels per truss for four alternate trusses.

Support wall displacements were measured to provide information on the truss boundary conditions. The RLRPs, similar to those used for vertical deflection measurements, were attached to the test frame and measured the movement of the bearing plate in the horizontal plane as the trusses were loaded. As reported in Part I, those measurements had been taken using a dial gauge that, for safety reasons, limited the readings to the design load range of the assembly.

Deformations of the MCPs were measured for both single truss and full assembly tests. For these

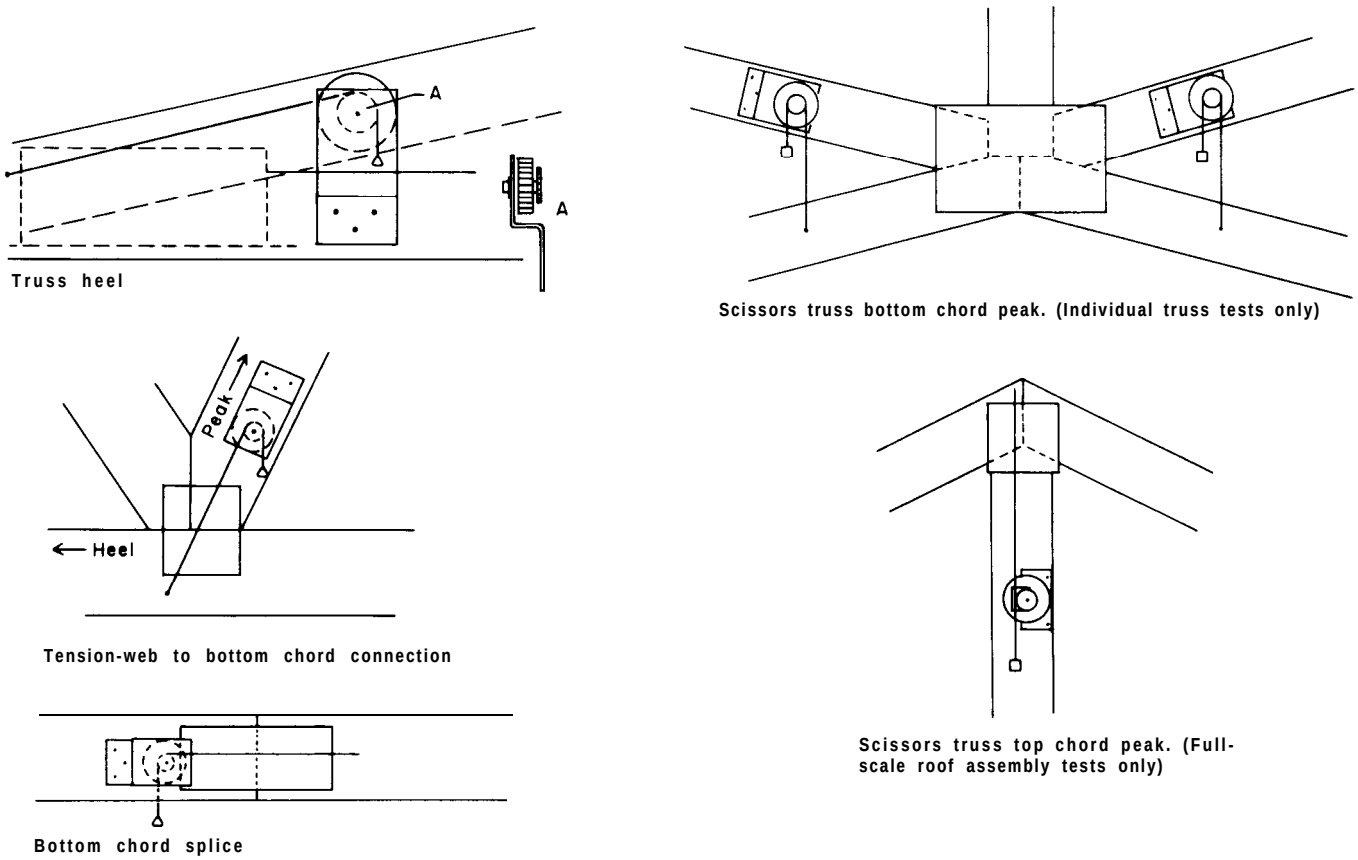

Figure 5—Truss joint displacement measurements taken for individual truss failure tests and two trusses in each assembly. (ML90 5401)

measurements, RLRPs with a 2-in. range and an accuracy of ±0.5 percent were attached to trusses as shown in Figure 5. They measured axial displacement at web-chord and bottom-chord splice connections, shear in heel connections, and rotation in the scissors bottom peak web-to-cord connection. Measurements were taken at (1) heel joints for all configurations, (2) tension-web to bottom-chord and bottom-chord splice connections for the Fink configurations, and (3) bottom-chord peak connection for the scissors configuration in both the individual truss and full assembly tests. These measurements were taken for individual trusses tested to failure and the fifth and eighth trusses from the west end in the full assembly tests.

Test Procedure

Tests were conducted in three phases. The first phase evaluated individual truss performance. The second phase tested the performance of each truss in the assembly loaded several ways. The third phase measured the stiffness and strength of the fully loaded assembly.

Individual Trusses

The purpose of the individual truss tests was to determine the stiffness of each truss and provide some basis for judging the load capacity of each truss configuration. Of the 12 trusses fabricated for each configuration, 4 were tested to failure and 8 were tested for stiffness in the individual truss loading setup.

As each truss was prepared for testing, it was given an ID and was inspected for fabrication quality. A three-character ID was used to assist in the organization of data files. The first character differentiated individual truss tests (T) from system truss tests (S). The second character designated the truss configuration (3 or 6 for Fink and S for scissors). The third character was a test sequence identifier (1-9 and A-C). The truss inspection concentrated primarily on the quality of the joints. Characteristics surveyed included plate placement, embedment, joint gaps, and lumber defects in the area of the connection.

Plate placement was evaluated on the basis of a translational misalignment of the centroid of the plate with respect to the center of the joint. These measure-

ments were taken at all heel and peak joints and at the tension-web to bottom-chord joints for the Fink trusses. Mislocations were measured in directions parallel-to-the-principle axes of an ideally placed plate using transparent templates. Plate rotations were not recorded unless they appeared to vary more than +5°.

Gap measurements focused primarily on heel and peak joints. For the Fink trusses, readings were also taken at the compression-web to bottom-chord joints. All measurements were recorded as the average gap measured along the member thickness (1-1/2 in.) dimension. At heel connections, readings were taken at points where the top and bottom surface of the bottom chord intersected the top chord. At peak connections, readings were taken only at the top because the bottom of the top chords was not accessible. Joint gaps and MCP misplacements are discussed further in Appendix C.

Individual trusses tested to determine relative stiffness were loaded to DSN. Loads up to DSN were applied in increments of 0.25 × DSN and held for 1 min at each load step to assure pressure equilibrium and a static condition prior to scanning the reaction and deflection channels. After testing, these trusses were used to construct the roof assemblies.

The individual trusses tested to failure were first loaded to DSN and then unloaded the same as the trusses tested only for stiffness. They were then loaded a second time, beginning with a ramp load to the design value. Loads were then increased in increments of 0.25 × DSN up to 2.5 × DSN, and then the trusses were continuously loaded to failure. Reactions and deflections were scanned continuously during final loading.

Roof Assembly Stiffness Tests

Before any loads were applied to the roof assembly, the reactions were adjusted to give a uniform distribution of the dead load. When the load cells were first placed under the truss reactions, we found that the reaction forces ranged from 30 to 500 lb. By adjusting the heights of the reaction post in the center of each load cell, we were able to narrow this range from 180 to 220 lb. The difficulty of adjusting to a range of less than 40 lb did not appear to be worth the added effort.

Roof assembly stiffness tests were conducted in three parts. First, each truss was loaded individually in the assembly to evaluate the influence of truss location and stiffness on load distribution. Second, sections of the roof were loaded to see how the assembly responded to nonsymmetrical loads. Third, the full assembly was loaded.

Tests of trusses loaded individually in the assembly were conducted following the same procedure as that used for trusses tested to DSN outside the assembly. As load was applied, reactions were measured for all trusses in the assembly to characterize load influence of each truss assembly. To evaluate the effect of nail spacing, each truss was tested twice, once with sheathing nailed 12 in. on center and again with end nails spaced 6 in. on center.

For each Fink assembly, the fifth truss was tested twice to DSN to evaluate the effects of bearing plate horizontal restraint. For the initial 3:12 Fink assembly, a cable was used, attached to opposing bearing plates close to the fifth truss, along with an attached load cell to monitor horizontal thrust. After completing the series of individual truss tests, this cable was removed, and the fifth truss was retested with the bearing plate allowed to move within the restraint imposed by the sheathing attachments. For the 6:12 Fink assembly, the bearing plates under the fifth truss were allowed to move freely during the initial set of individual assembly truss loadings. After these tests, the bearing plates were constrained in the channel attached to the triaxial load cells, supporting the bearing plate under this truss to measure its horizontal reactions.

After each truss was tested, a uniform load was applied, first to half the roof and then to the entire roof. During the full-span loading, the first eight trusses in the assembly were loaded. The gable end was not loaded directly. Each assembly loading sequence started at the dead load and increased in increments of 0.25 × DSN until the assembly reactions summed to DSN for the eight loaded trusses.

Full Assembly Loaded to Failure

Only the inner seven trusses were subject to direct loading during the full assembly failure tests. The loads were applied in increments of 0.25 × DSN, with a 1-min pause between scans. When loads exceeded 2.0 × DSN, the data were scanned continuously to detect any failures that might occur between target load levels.

Results

This study evaluated construction materials and three roof assemblies. Primary emphasis, however, was placed on the structural performance of the roof assemblies. A summary of the material property evaluation is in Appendix A. Roof assembly test results include the stiffness and strength of individual trusses, the distribution of loads within each assembly, and the strength and failure modes observed for the three assemblies.

Individual Trusses

Truss Inspection

No major defects or fabrication errors were noted for any of the trusses prior to testing. Joint gaps for the Fink configurations averaged under 1/16 in., with maximum readings in the heel joints ranging up to 3/16 in. Twenty percent of the gaps measured for the scissors trusses were larger than cited by TPI as a maximum tolerance limit, 1/8 in., but no gaps exceeded 3/16 in. Maximum MCP misplacements, expressed as a percentage of the corresponding connector plate dimension, were 10 percent for the Fink trusses and only 4 percent for the scissors. Average values were between 1 and 3 percent.

Truss Tests

Although stiffness tests gave no indication of physical damage to the trusses, the 3:12 Fink trusses did exhibit slightly nonlinear load deflection behavior when loaded to DSN (Fig. 6). This was attributed to tightening of gaps in compression joints and buckling of the top chord close to the heel joints. For subsequent truss tests, additional braces were added near the heels to prevent top-chord buckling.

Truss deflection profiles (Fig. 7) show that most of the vertical deflection occurred in the truss sections between the reactions and the first intersection of the chord and web element (node point). The small difference in the vertical deflections measured between the two top nodes and the peak suggests that any of these readings or the average of the three readings can indicate global truss deflection under uniformly distributed load.

Table 1 lists individual truss ultimate loads and failure modes. The Fink trusses exhibited consistent ultimate strengths limited by failures at the heel connection. The scissors trusses, however, had a much greater propensity for twisting and buckling of the top chord. Modifications of the bracing system to prevent top-chord out-of-plane deformations caused wider variation in these results than was obtained for the Fink trusses.

Heel connection failures were due primarily to in-plane shear. For seven of the eight Fink trusses, the MCPs deformed in shear, followed by plate tooth withdrawal from the chord. For Fink truss T61 and scissors truss TSA, however, twist in the top chord placed a transverse withdrawal force on the heel connection. Bracing added to restrain transverse force at the heel may have caused the failure mode to change for TSB. In this case, the peak buckled sideways. An out-of-square butt cut at the peak joint, giving wood contact on one surface and a 1/8-in. gap on the other, caused the peak

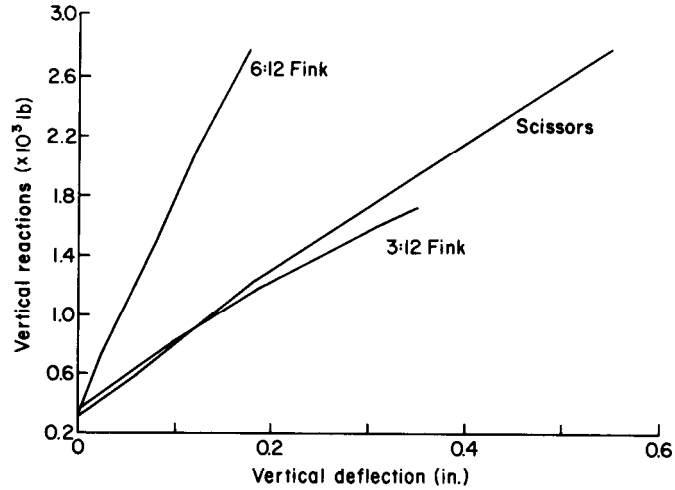

Figure 6—Load-deflection plots typical of the three truss configurations when tested individualy. (ML90 5391)

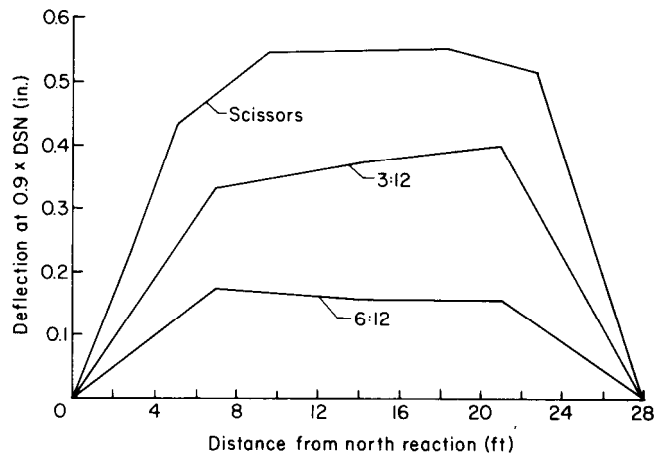

Figure 7—Individual truss deflection profiles for 3:12 Fink, 6:12 Fink, and scissors truss. (ML 90 5396)

to be pushed out of plane and the top chord to buckle. The final scissors truss, completely braced, failed when the king post pulled out of the MCP at the upper peak.

Shear displacements measured at the heel at maximum load were largest for the 3:12 trusses, with values as large as 0.25 in. For the 6:12 and scissors trusses, the largest heel displacement measured was 0.068 in. Bottom-chord splice joints and web-chord joints also exhibited large displacements (>0.03 in.), but no failures were at these joints. Finally, member rotation measurements at the bottom-chord peak joint of the scissors trusses were less than the range of significance of the RLRP used to measure them. The largest reading showed a decrease in the angle between the bottom chord and the web chord of only 0.003 radian.

Table1—Comparison of truss stiffness and strength tests conducted inside and outside the assembly

Assembly truss	Slope (lb/in)	Load (lb) Maximum Single	Load (lb) Maximum Assembly	Load (lb) Assembly maximum	Failure
3:12 Fink					
Gable				2,280	
T31	4,420	4,530			Heel connection-steel shear and pullout
T32	4,090	4,360			Heel connection-steel shear and pullout
T33	4,000		3,900	3,280	
T34	5,130		4,740	4,210	
T35	3,650		4,900	4,580	
T36	4,040		4,550	4,550	Wood bending-tension at knot
T37	3,990		4,280	4,260	
T38	4,160		3,610	1,780	Wood bending-tension at knot
T39	4,630	4,540			North heel plate failure
T3A	4,390		4,520	4,231	Wood failure-tension at knot
T3B	3,890	4,270			Shear failure of north heel plates
T3C	4,110		3,760	2,980	Steel failure-bottom chord splice
Average	4,210	4,430	4,280	3,570	
COV[a] (%)	9	3	10	25	
6:12 Fink					
Gable				2,960	
T61	10,220	4,460			Heel connection pullout-top chord twist
T62	14,140			4,290	No failure observed
T63	14,720		5,280	5,280	Tension web-bottom chord connection
T64	12,410	5,780			Heel connection-steel shear and pullout
T65	13,300		6,270	6,270	Tension web-bottom chord onnection
T66	14,610		5,920	5,920	Tension web-bottom chord connection
T67	14,830		5,340	5,340	Tension web-bottom chord connection
T68	13,990		5,850	5,800	Tension web-bottom chord connection
T69	15,220		6,340	5,720	Peak connection-tension web pullout
T6A	14,140		5,640	4,750	Bottom chord splice connection metal failure
T6B	12,940	5,880			Tooth pullout at the north heel
T6C	12,280	5,510			South heel plate pullout and shear
Average	13,570	5,410	5,810	5,150	
COV[a] (%)	10	10	7	19	
Scissors					
Gable				4,530	
TS8	4,510		4,070	4,070	
TS2	4,810		4,970	4,970	Crack at knot found after test
TS3	5,680		6,300	6,260	Top peak connection-plate pullout
TS4	5,090		6,600	6,180	
TS5	4,600		6,560	6,100	Top peak connection-plate pullout
TS6	5,920		6,950	6,950	Top peak connection-plate pullout
TS7	5,850		5,880	5,750	Top peak connection-plate pullout
TS1	6,160		4,560	2,240	Bottom peak connection-plate pullout
TS9	4,280	5,080			
TSA	4,880	4,890			Buckling of the north top chord
TSB	4,230	4,000			Buckling and twisting of top chord
TSC	4,690	6,900			Top peak connection-plate pullout
Average	5,060	5,220	5,740	5,230	
COV[a] (%)	13	20	17	26	

[a] Coefficient of variation.

Assembly Load Distribution

Distribution of loads within the roof assemblies was influenced by truss stiffness, truss location with pinned ends of the bearing plates and the gable end, and sheathing nail pattern. Load tests on individual trusses in each assembly provided a means of characterizing these influences. Section and full assembly loads provide a basis for evaluating the superposition of individual truss load effects.

Individual Truss Load

Figures 8, 9, and 10 show how loads were distributed from individually loaded trusses in each of the three roof assemblies. For example, a full-span load was applied to each truss individually and the resulting assembly reactions were recorded. The increase in the force measured at each reaction was then divided by the total load applied to the individual truss. Numbers shown in Figures 8, 9, and 10 indicate the percentage of applied load that was distributed to the truss at each location when an individual truss in the assembly was loaded. Several load levels within the design load range of the loaded truss showed little variation in the load distribution.

The magnitude of the distributed load varied with the location of the truss being loaded and the configuration of the trusses. For each assembly, a positive reaction response was measured for trusses up to five spaces away from the loaded truss; beyond that, the truss reactions indicated a negative or upward response. The scissors assembly displayed the greatest tendency to distribute load away from a loaded interior truss and the greatest tendency to distribute loads to the gable end and free-end trusses. Load distribution to the adjacent truss varied little with configuration, but the distribution of loads beyond three trusses away was greatest for the scissors assembly.

The free-end truss and gable end appeared to play a greater role in the performance of the scissors assembly than the Fink assemblies. Figure 10 shows how when the third or fourth truss from either end was loaded, reactions for the end truss or gable end were larger than those of the truss next to the end. In each case, this can be explained by the fact that load is transferred past the interior trusses to the relatively stiffer free-end trusses and the gable end. Loads carried by diaphragm action of the sheathing caused the intermediate scissors to spread as they deflected, but the gable end resisted horizontal and vertical displacement.

An anomaly of the scissors assembly was a larger deflection measurement for the free-end truss than the second truss when either the second, third, or fourth truss was loaded. The gable end stiffness in the horizontal plane reduced spreading as a result of forces distributed through the bearing plate and sheathing diaphragm for trusses on its end of the roof. This resulted in an increasing tendency for spreading with distance from the gable end. One explanation for the increased reactions and larger deflections of the end truss is that a slightly heavier outward force caused it to spread more than the second truss and, thus, to have a slightly larger peak deflection. As the end truss deflected as a result of spreading, the overhang rotated upward into the sheathing and picked up load from the second truss reactions.

In each phase of the assembly tests, horizontal displacement measurements taken along the bearing plates gave some indication of how the importance of this restraint varies with system configuration. In all cases, vertical load on an individual truss resulted in an outward thrust on the bearing plate at its point of connection. Under individual truss loading, the largest bearing plate spread occurred on the free end of the roof; however, under full assembly load, the spread in the middle of the roof was slightly larger than at the west end. At design load on the full assembly, the maximum spread was about 0.3 in. for the scissors assembly, 0.10 in. for the 3:12 assembly, and 0.03 in. for the 6:12 assembly. The bearing plate stiffness and truss connection to the bearing plate obviously had major impacts on load distribution.

Assembly Loads

Variations in truss deflection under full assembly load were influenced more by assembly interactions and truss location with respect to the gable end than by relative truss stiffness. Figure 11 shows the deflection profiles for the three roof assemblies under uniform assembly DSN load. In each case, the load was applied directly to the eight trusses and distributed to the gable end. Each profile shows the same pattern of truss deflection increasing with distance from the gable end with little variation as a result of relative stiffness. The gable-end influence on truss deflection appears to be smallest for the 6:12 roof and largest for the scissors roof.

The smooth pattern of truss deflections combined with variations in truss stiffness resulted in **a** slightly erratic pattern for truss reactions (Fig. 12). Although a relatively stiff truss is limited to less deflection than a limber truss, it may still pick up a larger share of the assembly load. The truss reaction patterns for the 6:12 and scissors assemblies shown in Figure 12 demonstrate this effect.

Assembly Strength

Table 1 compares individual truss and full assembly ultimate loads. In the majority of cases, ultimate

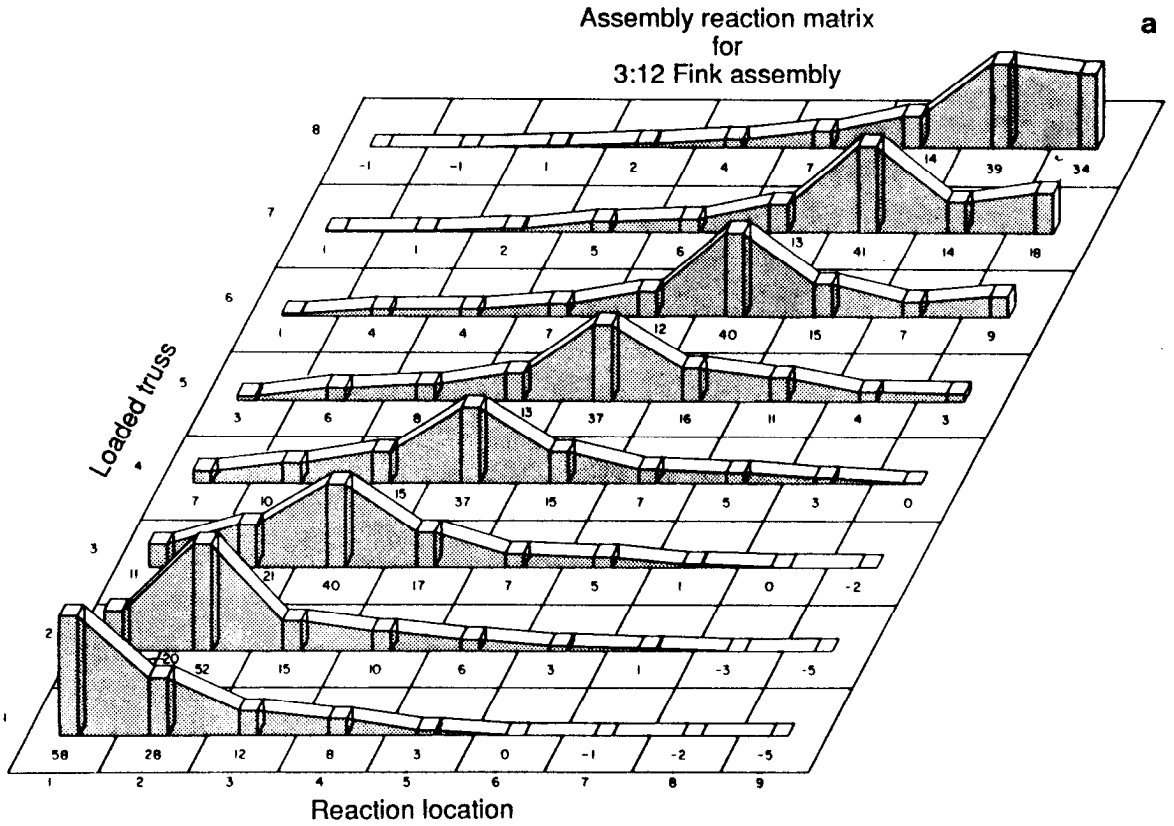

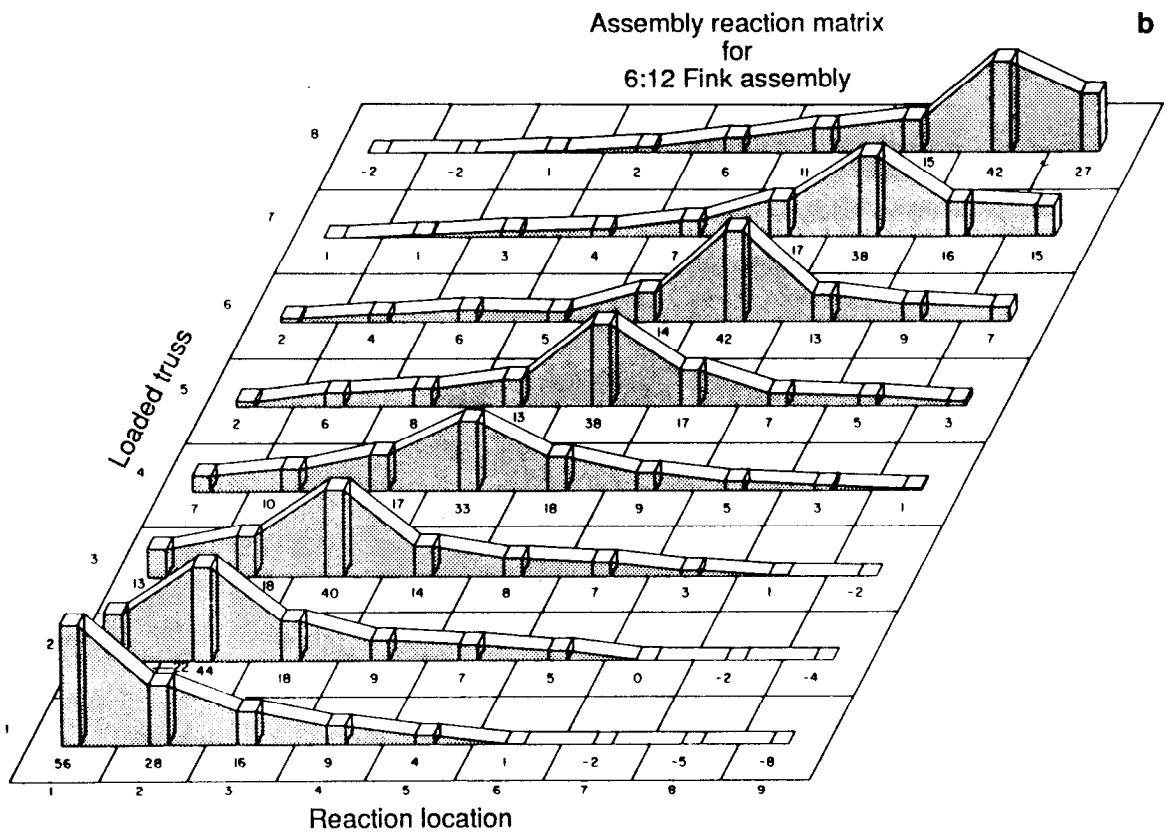

Figure 8—Load influence matrices *for the 3:12 Fink* (a) and *6:12 Fink (b) and scissors roof (c) assemblies. Load distribution in each* case *is expressed* as *a percent of the* total *applied* load *that is picked up by each truss in the assembly. (ML88 5372, ML89 5545, ML89 5546)*

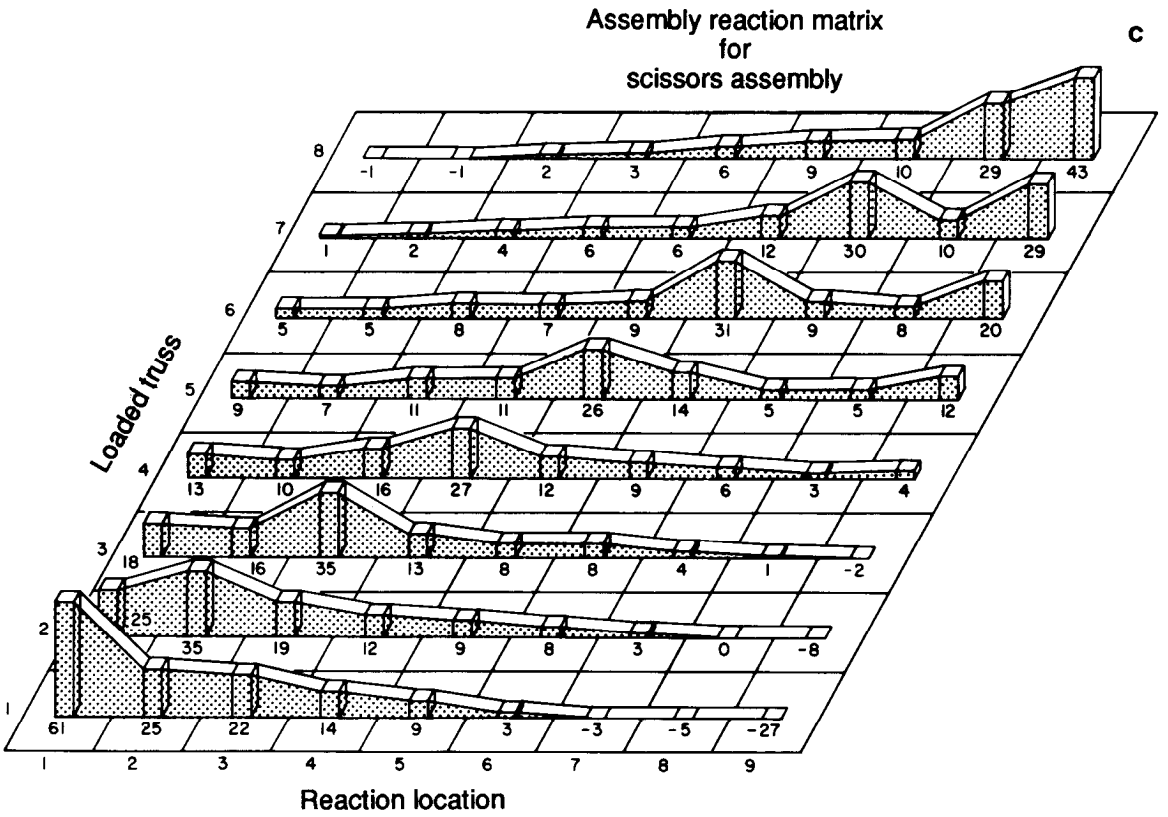

Figure 8—con.

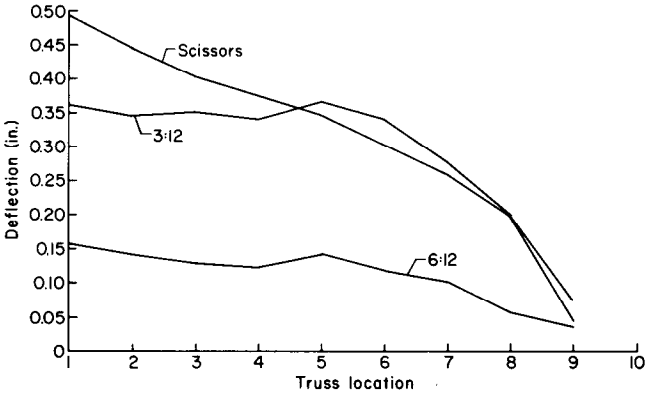

Figure 9—Deflection profiles for the 3:12 Fink, 6:12 Fink, and scissors roof assemblies. Plots compare truss deflections when the assembly was loaded to DSN. In this case, the DSN load was applied to each truss in the assembly, and no load was applied to the gable end. (ML90 5386)

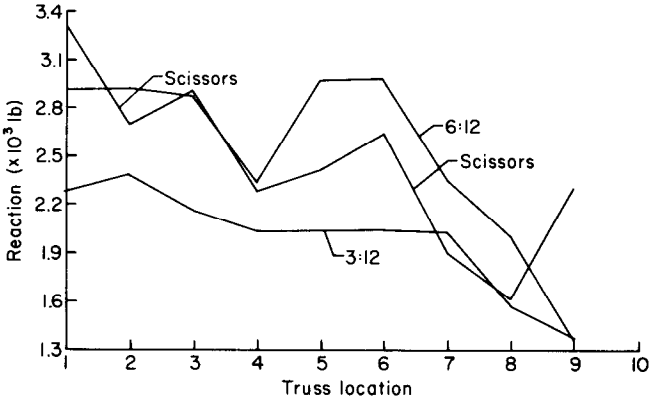

Figure 10—Reaction profiles for the 3:12, 6:12, and scissors roof assemblies. Plots compare the distribution of assembly loads for the three roof configurations when each was loaded to its DSN value. The DSN load was uniformly applied to each truss in the assembly. No load was applied to the gable end. (ML90 5390)

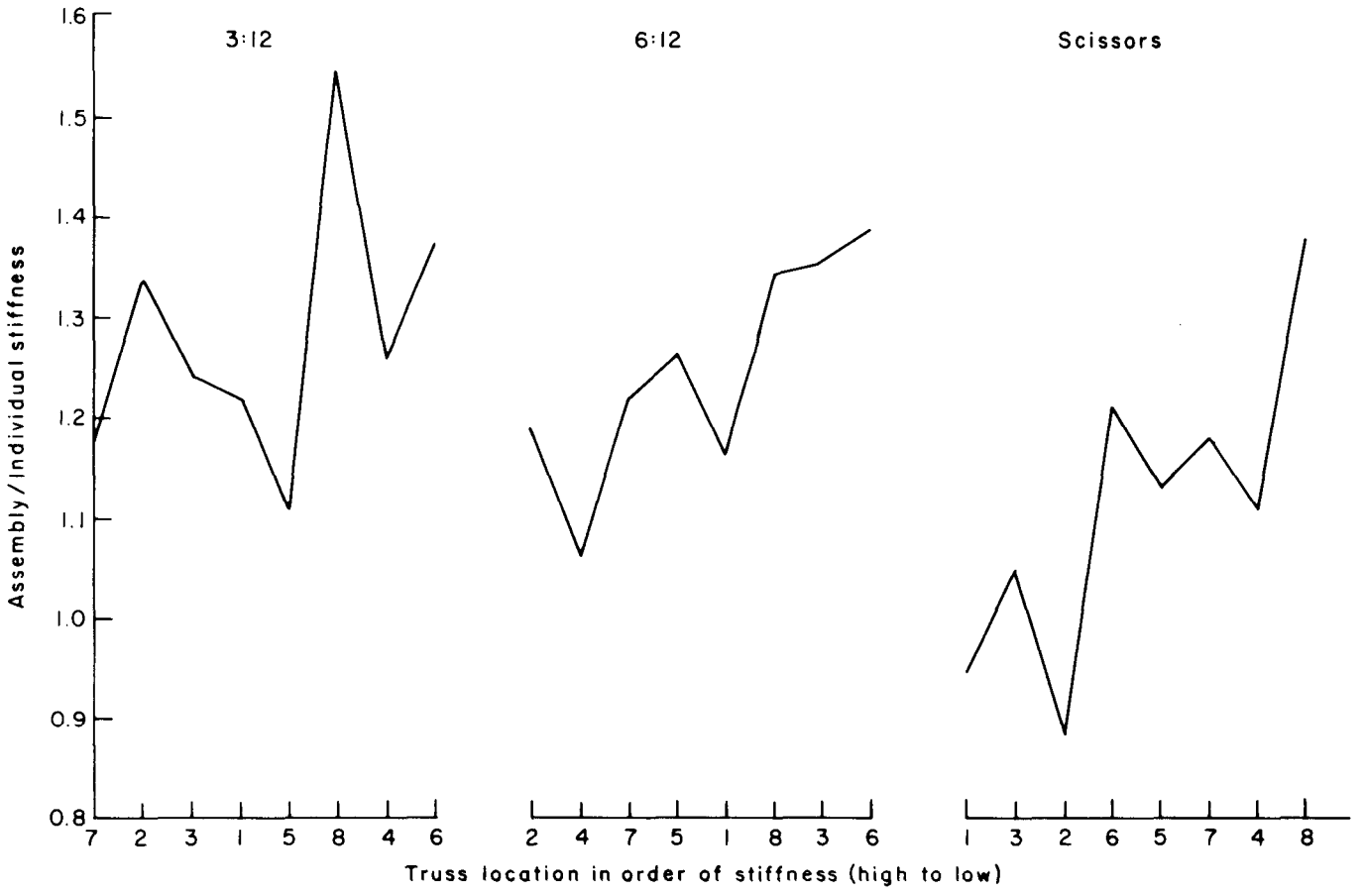

Figure 11—Assembly effects on apparent truss stiffness. Stiffness, expressed as the sum of truss reactions divided by vertical deflection, is larger in the assembly due to sheathing-chord interaction and load redistribution to stiffer members. (ML90 5385)

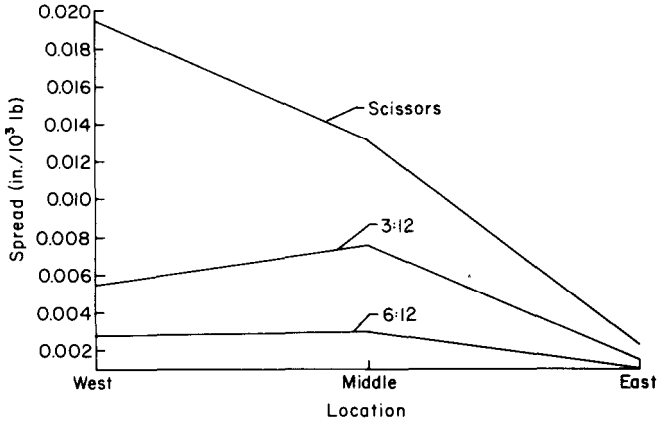

Figure 12—Bearing plate spread measured under full assembly load. Sum of displacements of the north and south bearing plates regressed on assembly load to give bearing plate spread in inches per thousand pounds at each of three locations. (ML90 5395)

truss loads occurred after the maximum assembly load was reached. For the 3:12 Fink assembly, one truss (T38) reached its ultimate strength before the maximum assembly load and carried less than half its ultimate load when the assembly maximum load was recorded. The scissors assembly had two trusses (T51 and T57) that reached ultimate load before the maximum assembly load. Truss T51 reached its maximum load 2-1/2 min and 501 lb before the maximum assembly load. For truss T57, ultimate load was recorded 8 s before the maximum assembly load. The 6:12 Fink assembly had five trusses reach their ultimate load at the same time as the maximum assembly load, compared to two trusses in each of the other two assemblies.

The failure modes, compiled in Table 1, indicate a prevalent failure mode for each of the three configurations. The majority of 3:12 Fink assembly failures were due to combined bending and tension in the bottom chords. The 6:12 Fink failures were almost exclusively a result of tension-web pullouts at connections. Five of these pullouts occurred at the bottom-chord connection. The scissors assembly failures were king post pullouts at the upper peak. When one of these prevalent failures occurred, loads were apparently redistributed to the same critical location on adjacent trusses. Thus, adjacent trusses have a tendency to fail in the same mode. This was confirmed by the rapid failures of adjacent trusses in the 6:12 and scissors failure tests.

Horizontal displacements, sheathing-chord slip, and joint deformation measurements for the load to failure are given in Appendix B.

Analysis of Results

The objectives of this study were to evaluate assembly interaction effects and to provide a basis for development and evaluation of assembly analytical models. Factors considered in evaluating interaction effects include stiffness, strength, and failure mode of individual trusses and roof assemblies. In each case, the evaluation relies on a comparison of individual truss and full assembly performance. To enhance the analysis, reference is made to the Part I report (Wolfe and McCarthy 1989) that dealt with an extreme truss stiffness variability, a bias toward wood failure, and symmetrical roof assemblies tested without the influence of a gable end. In this study, truss stiffness variation is representative of that found in a conventionally built light-frame trussed roof assembly. No attempt was made to bias the failure mode, and the roofs were constructed with a gable end.

Truss Stiffness

Truss stiffness is primarily a function of the lumber stiffness. Joint displacements also influence truss stiffness. However, within the linear range of truss performance, truss deflection as a result of joint strain is small in comparison to the strain in the wood members. For the trusses used in this study, lumber came from a single source and was assigned to individual trusses by the truss fabricator with no prearranged assignments. The average truss member MOE within a given configuration ranged from 1.89×10^6 lb/in^2 for the 6:12 trusses to 1.92×10^6 lb/in^2 for the 3:12 trusses; COV ranged from 18 to 19 percent. The average truss member MOE range from 1.57×10^6 to 2.31×10^6 lb/in^2; COV ranged from 4 percent for the scissors to 10 percent for the 3:12 Fink trusses. Truss member MOE values are given in Appendix A.

The slopes of the truss load-deflection plots (Table 1) are referenced as a measure of truss stiffness. The deflection value used to determine this slope was the average of the three node-point values. This is supported by the observation that truss deflection profiles (Fig. 7) appear relatively flat, with some slight variations as a result of localized displacements over the center portion of the truss. A least squares linear regression was used to determine the slope of the sum of the truss reactions compared to this average node deflection.

Table 2 gives three stiffness values determined for each truss used in a roof assembly. In each case, the stiffness values were determined as the slope of the plot of measured reactions compared to measured deflections. On the average, truss stiffness variability is less than half that measured for the lumber. Naturally, this varied with the truss configuration. Lumber stiffness COVs for the three assemblies ranged from 18 to 19 percent. Individual truss stiffness COVs ranged from 4 to 11 percent. The higher COV determined for the 3:12 configuration is primarily from the high stiffness measured for one truss (T34). Without that truss, the COV would have been 5 percent. For the scissors trusses, the higher COV reflects a true spread in the stiffness distribution.

Assembly Effects

The Part I report (Wolfe and McCarthy 1989) identified two assembly interaction mechanisms-composite action and load sharing-that act to improve the apparent performance of trusses in an assembly over that exhibited in individual tests. Composite action is defined as the interaction between the truss and the roof sheathing that serves to increase the stiffness of the top chord and thus of the truss. Load sharing is defined as

Table 2—Truss stiffness values determined as the slope of the load deflection curve for trusses tested individually tested individually with those determined for trusses loaded as part of the assembly

Roof assembly	Stiffness value (lb/in deflection)										Coefficient of variation (percent)
	Truss location, west end								Gable end	Average	
	1	2	3	4	5	6	7	8			
3:12 Fink											
Individual	4,110	4,390	4,160	3,990	4,040	3,650	5,130	4,000		4,184	10
Assembly A[a]	4,880	5,650	4,950	4,610	4,250	4,780	5,700	5,660	23,590	5,060	10
Assembly B[b]	5,010	5,870	5,160	5,020	4,470	5,010	6,000	6,190	23,660	5,343	11
(Ratio A/individual)	(1.19)	(1.29)	(1.19)	(1.16)	(1.05)	(1.31)	(1.11)	(1.42)		(1.18)[c]	
(Ratio B/individual)	(1.22)	(1.34)	(1.24)	(1.26)	(1.11)	(1.37)	(1.17)	(1.55)		(1.24)	
6:12 Fink											
Individual	14,140	15,220	13,990	14,830	14,610	13,300	14,720	14,140		14,369	4
Assembly A	14,060	18,240	18,590	15,360	17,990	18,190	16,690	17,330	29,130	17,056	9
Assembly B	16,440	18,140	18,970	15,760	18,480	18,440	17,970	19,010	26,520	17,901	6
(Ratio A/individual)	(0.99)	(1.20)	(1.33)	(1.04)	(1.23)	(1.37)	(1.13)	(1.23)		(1.18)	
(Ratio B/individual)	(1.16)	(1.19)	(1.36)	(1.06)	(1.26)	(1.39)	(1.22)	(1.34)		(1.24)	
Scissors											
Individual	6,160	5,850	5,920	4,600	5,090	5,680	4,810	4,510		5,328	11
Assembly A	5,540	5,110	6,060	4,830	5,570	6,830	5,510	5,780	18,770	5,654	10
Assembly B	5,820	5,170	6,220	5,100	5,760	6,890	5,680	6,220	18,320	5,858	9
(Ratio A/individual)	(0.90)	(0.87)	(1.02)	(1.05)	(1.09)	(1.20)	(1.15)	(1.28)		(1.04)	
(Ratio B/individual)	(0.94)	(0.88)	(1.05)	(1.11)	(1.13)	(1.21)	(1.18)	(1.38)		(1.07)	

[a] Assembly A was constructed with sheathing end nailing spaced 12 in. on center.
[b] Assembly B was constructed with sheathing end nailing spaced 6 in. on center.
[c] Average ratios do not include values for the eighth truss as a result of influence of gable end.

an assembly attribute resulting from boundary conditions that force all trusses in the assembly to deflect together. This then serves to distribute a greater share of the load to stiffer trusses and to reduce the apparent variability in truss stiffness determined using tributary area loading assumptions.

Our assessment of roof assembly interactions assumes that composite action provides the same stiffness increase for each truss but no increase in strength. Composite action stiffness increase is primarily an increase in effective moment of inertia of the top chord of the truss. Conventional truss design assumes little or no variability in top-chord or connection stiffness. A truss designer would therefore expect little variability in the effect of composite action on truss stiffness. As loads approached the roof assembly capacity, sheathing-chord slip measurements (App. B) showed that the nailed connections had been loaded well beyond the 0.015-in. limit for their desired design values. Although they continued to transfer load between the trusses and the sheathing, these connections were no longer rigid enough to provide composite action between the truss chords and the sheathing. Therefore, we feel that the composite action that provides an initial increase in chord stiffness diminishes with increased truss deflection to the point that it does not provide a significant increase in truss load capacity.

Load sharing, on the other hand, would be expected to vary widely with relative stiffness of trusses within a given assembly and its effects would increase as load approaches the assembly capacity. If load sharing is viewed as a transfer of load, either through plate or diaphragm action of the sheathing, from limber to stiffer trusses, its effect would be to increase load for stiffer trusses and decrease it for limber trusses. Load sharing depends on the stiffness and span of the sheathing as well as relative deflection of adjacent trusses. Load sharing does not occur until one truss deflects relative to adjacent trusses. This may be due to truss stiffness variation, plastic deformation in a connection, or partial failure of a chord member. The load that is shed will increase with relative displacement, an increase in the relative stiffness of the sheathing, and a decrease in the truss spacing.

For simplicity, our evaluation of composite action and load sharing attempts to support the premise that these two effects are mutually exclusive. Composite action initially serves to increase the effective stiffness of the trusses, but it then diminishes as the trusses are loaded beyond design load. Load sharing influences the variability in effective truss stiffness by enforcing boundary conditions that limit relative displacement, and it influences assembly load capacity by shifting load away from the weakest link.

Composite Action

Average truss stiffness ratios (Table 2) are attributed to composite action. These values indicate the stiffness increase for trusses loaded within the range of design load in the assembly compared to trusses outside the assembly. To isolate the composite action effects from load-sharing effects, average truss stiffness values were calculated, excluding the ratio measured for the eighth truss. In each case, the gable end appeared to have a strong effect on limiting the vertical deflection of the eighth truss. This effect was attributed to load sharing rather than composite action. For the 12-in.-nail spacing, the Fink assemblies showed a composite action effect of 18 percent, and the scissors assembly showed an effect of only 4 percent. The addition of nails at 6-in. intervals increased truss stiffness 6 percent for the Fink and 3 percent for the scissors trusses.

Although the 6:12 Fink trusses were initially three to four times as stiff as the 3:12 Fink trusses, the effect of composite action was the same for both assemblies. Because the sample plywood, connections, and truss spacing were the same for both assemblies, a greater stiffness increase would be expected for the 3:12 assembly. The measured deflections, however, were dependent on sheathing stiffness about a horizontal axis. Thus, the effective stiffness contribution of the plywood increased with slope. In either case, composite action was limited by connection stiffness, which was assumed to be the same for the two assemblies.

A comparison of individual truss failure loads inside and outside the assemblies suggests that composite action has little or no effect on the strength of trusses used in an assembly. When we compared the load capacity of trusses tested outside the assembly to that of trusses tested as part of the assembly, we found no difference at the 0.05 significance level for any of the truss configurations. The strength of this conclusion is limited because of the small sample of trusses tested individually. However, it is reasonable to assume that as a truss approaches its ultimate strength in the assembly, the sheathing connections begin to behave plastically in the area of greatest stress, and they will contribute little to stress reduction on the critical truss member. Thus, average truss failure loads determined from individual tests and those tested in the assembly were combined to give the truss failure loads reported in Table 3.

Load Sharing

Load-sharing mechanisms serve to decrease apparent truss stiffness variability and increase roof load capacity. Limber trusses receive greater support as a result of load sharing than the stiffer trusses, decreasing apparent stiffness variability in the assembly. Load-sharing mechanisms also distribute load away from partially damaged trusses, allowing them to continue to contribute to assembly load carrying at a decreased level.

The variation in relative deflection from midspan to the truss reaction causes load-sharing mechanisms to have an apparent effect on truss stiffness. A vertically loaded truss deflects horizontally and vertically. The horizontal displacement and rotation over the bearing point causes the truss to pick up load at the reaction, and the vertical displacement at midspan causes it to shed load through plate and diaphragm action of the sheathing. Therefore, a relatively limber truss appears to be stiffer as a result of these increased reaction forces. This same mechanism causes the stiff truss to lose some reaction force, making it appear to have less advantage as a result of composite action.

The nonsymmetric nature of the roof assemblies resulted in some variation in assembly effects with truss location. Variations in truss stiffness were not as pronounced in this study as those reported in Part I (Wolfe and McCarthy 1989); therefore, load distribution away from limber trusses was not as apparent. For the first five trusses from the open end, composite action may have played a greater role in the assembly influence on truss stiffness than on load distribution. Those trusses close to the gable end exhibited increased stiffness as a result of load sharing with the gable end. Figure 13 shows how the ratio of assembly stiffness to individual truss stiffness varied with relative truss stiffness and location in each roof assembly. In each case, truss location, designated as its position number (1 to 8) with respect to the free end of the roof, was arranged in order of relative truss stiffness (high to low). Although there appeared to be a trend of greater benefit for the limber trusses, variation in truss boundary conditions makes it difficult to isolate. In each case, the most limber truss in the assembly showed a stiffness increase of more than 30 percent, and the stiffest truss increase was less than 20 percent. For the scissors assembly, the stiffest truss showed a 6 percent lower stiffness than when tested individually.

For the scissors assembly, the ratio of assembly/individual truss stiffness showed a definite increase from the open end to the gable end (Fig. 13). This was primarily due to the arrangement of the trusses in which the limber trusses were located close to the gable end, which had a much larger relative stiffness in the scissors assembly than in either of the Fink assemblies. In addition to providing support against vertical loads, the gable end provided extra restraint against lateral spread of truss reaction points. This restraint on one end of the assembly resulted in a tendency for horizontal displacements to increase toward the open end (Fig. 14). The

Table 3—Evaluation of the inherent load-sharing factor for three roof assemblies

Truss type	Weakest truss maximum load[a] (lb)	Tributary area load at failure (lb)[b]				Load-sharing increase (percent)			
		1	2	3	4	1	2	3	4
3:12 Fink	3,610	4,590	4,280	4,020	3,900	27	19	11	10
6:12 Fink	5,280	6,620	6,180	5,790	5,780	25	16	9	9
Scissors	4,560	6,720	6,280	5,880	5,670	47	37	28	24

[a] Lowest maximum load measured for a truss that failed when loaded in the roof assembly.

[b] 1—seven loaded trusses are assumed to carry total applied load.
2—free-end trusses carry half the tributary area load of the seven loaded trusses.
S-free-end truss and gable end each carry half tributary area load of the seven loaded trusses.
4-neglect the gable end reactions in calculating total load on the assembly and assume free-end truss carries half the load of each of the seven loaded trusses.

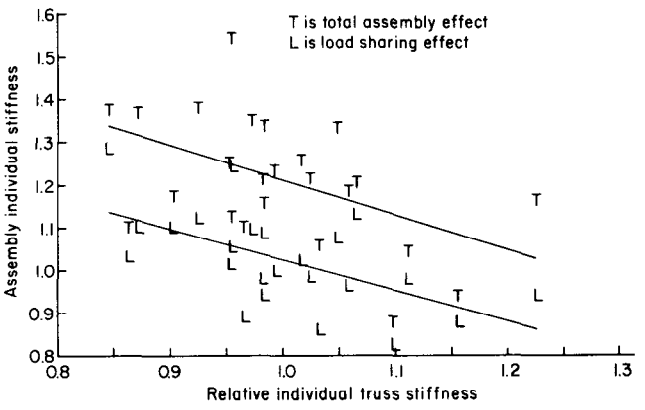

Figure 13—Assembly effects on truss stiffness. Plot of assembly individual stiffness ratios for all trusses tested in the three assemblies compared to relative individual truss stiffness within each assembly. (ML90 5397)

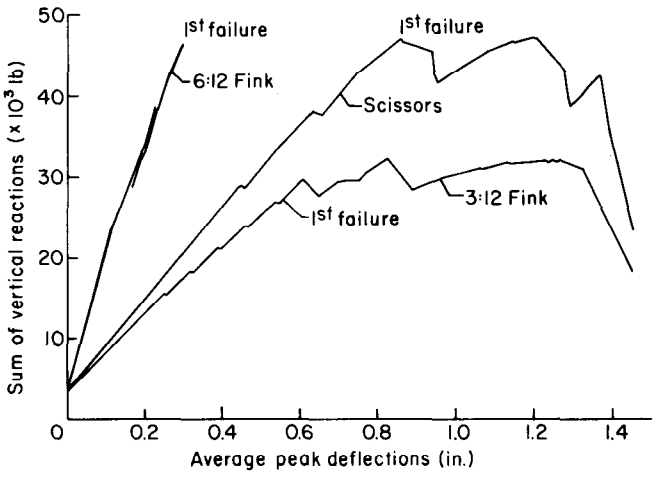

Figure 14—Maximum load-failure sequence. After each failure, assembly load dropped off. Upon reloading, subsequent failures occurred at load levels close to that of the first failure. (ML 90 5392)

combination of increased load and decreased horizontal restraint caused trusses on the open end to appear less stiff in the assembly than they did when tested individually.

The load-sharing increase for stiffness was estimated by factoring out composite action effects from the total assembly stiffness increase determined for each truss. Using the tributary area or as-loaded assumption for estimating truss stiffness gave an unrealistically large advantage to those trusses close to the gable end, so truss stiffness values were evaluated solely on the basis of measured reactions. Composite action was characterized as the average stiffness increase (Table 2), leaving load sharing to account for variability about the average. Figure 13 shows how the total assembly effect and load sharing varied with relative truss stiffness within an assembly.

Figure 13 is a composite of the assembly/individual stiffness ratio compared to relative individual truss stiffness for the three roof assemblies tested. The scatter in these data was due in part to the effects of the gable end that partially overshadows the load-sharing effects as a result of relative truss stiffness and behavior variations between the Fink and scissors truss. The data were derived using least squares linear regression to show the general trend. These results

suggest that for a truss stiffness COV of 10 percent within a roof, the average truss would be expected to show 20 percent less deflection (strain) at a given load in the assembly than outside the assembly.

Roof assemblies and individual trusses are normally assumed to be weak-link structures for purposes of design. Conventional truss design focuses on the ratio of induced stress to expected strength for each member. The expected member strength value is the estimated near minimum value for the global population of lumber in the specified grade and species. As a result, the truss design load capacity is assumed to represent a minimum value for all trusses made using similar material and the same configuration. If a truss is to be used in a repetitive member assembly, a 15-percent increase is allowed for member bending stress, but the weakest truss is still assumed to dictate the roof load capacity. This approach ignores the existence of a mechanism by which loads may be distributed around areas of local weakness.

In this study, load sharing increased the assembly load capacity range from 9 to 47 percent, depending on assembly configuration and the assumptions used to evaluate tributary area truss load in the assembly. Using the values in Table 1, we derived the load-sharing strength increase as the ratio of maximum assembly tributary area load to weak-link-truss maximum load. As a result of differences in the boundary conditions, especially evident in the scissors trusses, the weak-link truss was selected from those that failed in the assembly rather than those trusses tested individually to failure. The tributary area loads were calculated in four ways to show the sensitivity to loading assumptions. Resulting values of weak link, tributary area load capacity of the roof assembly, and the corresponding load-sharing factors are given in Table 3.

The weak-link values were representative of truss design values without load duration and factor of safety adjustments. Dividing the weak-link maximum loads by their respective design values gives values of 2.06, 2.48, and 2.14 for the 3:12, 6:12, and scissors trusses, respectively. This is close to the duration of load and factor of safety adjustment used for lumber bending and tension stresses (2.1) and greater than that used for compression (1.9) (ASTM 1981a). Thus, the TPI design load derivation appears to be a reasonable weak-link predictor.

Four estimates of tributary area load cover a range of interpretations of load distribution in an assembly that includes trusses of identical stiffness. Estimates 1 and 2 assume that the gable end represents an assembly boundary condition that is part of the overall assembly effect. Estimate 1 assumes that only those trusses that are loaded directly in the assembly carry load. In this case, the maximum assembly load was divided by 7. Estimate 2 assumes that the free-end truss carries 1/2 the load carried by each of the other trusses. Estimate 3 attributes 1/16 of the total load to the gable end as well as the free-end truss and 1/8 of the load to each of the interior trusses. Estimate 4 is the same as estimate 2 except that the load distributed to the gable end is not included in the maximum assembly load.

Appendix D gives a similar evaluation of truss tests that were presented in the Part I report (Wolfe and McCarthy 1989). In that study, the truss design load provided a conservative estimate of weak-link truss load capacity as a result of using heavy gauge plates. The resulting load-sharing increase values determined for those trusses ranged from 13 to 29 percent for the 3:12 assembly and 30 to 49 percent for the 6:12 assembly.

Values shown in Table 3 support the use of a load-sharing increase for load capacity of trusses designed following TPI procedures and used in a repetitive member assembly. In two of the three cases, weak-link maximum load occurred before assembly maximum. In all cases, the weak-link load capacity was less than the assembly tributary area load. Therefore, a design procedure that attempts to predict assembly tributary area load capacity on the basis of weak-link individual strength values should be able to recognize a benefit to assembly load sharing.

Distribution of Loads Within an Assembly

We found that the most convenient way to characterize load distribution in the roof assembly was to express the sum of reactions for each truss in terms of the percentage of total assembly load. Reactions expressed in this manner exhibited little variation with load level. Thus, the load distribution pattern expressed in this manner was taken to be characteristic of the assembly.

We characterized the assembly load distribution pattern by measuring assembly response to the load placed on each truss. This approach provided the basis for evaluating the importance of truss relative stiffness and location. The resulting load distribution for each assembly can be expressed as the sum of influences of each truss loaded individually. Individual truss load influence on assembly reaction is shown for the three roof assemblies in Figures 8, 9, and 10. Superimposing assembly responses to loads on each truss gives an estimate of how loads are distributed when the full assembly is loaded. Table 4 compares the superposition prediction to measured response when all trusses are loaded simultaneously.

Table 4—Average load carried by each truss in the full assembly

Truss	Load (percent)[a]			
	6-in. nail spacing		12-in. nail spacing	
	Predicted	Measured	Predicted	Measured
3:12 Fink				
T3C	12.5	12.5	12.7	12.9
T3A	15.0	14.2	15.2	14.1
T38	12.1	12.4	12.9	12.2
T37	12.4	11.8	11.5	11.5
T36	11.1	11.2	11.8	11.1
T35	11.5	11.9	11.7	12.2
T34	11.0	11.3	12.7	11.9
T33	7.7	8.2	6.6	8.5
T31	6.6	6.4	4.7	5.6
6:12 Fink				
T6A	12.4	13.3	11.1	12.4
T69	13.7	13.3	13.2	13.7
T68	13.5	13.2	13.1	13.1
T67	11.0	10.2	10.7	10.3
T66	12.7	13.4	13.0	13.6
T65	13.4	13.6	14.1	13.8
T63	9.8	10.5	11.6	10.9
T62	8.7	8.6	8.8	8.8
T61	4.8	3.9	4.4	3.3
Scissors				
TS1	16.3	15.7	13.9	15.0
TS7	12.4	12.6	12.3	12.6
TS6	14.6	13.5	14.0	13.4
TS5	11.6	10.4	11.2	10.3
TS4	10.6	11.0	10.8	11.2
TS3	11.5	11.8	11.9	12.5
TS2	7.9	8.2	8.8	8.7
TS8	6.3	6.7	6.7	7.0
T61	8.8	10.1	10.4	9.3

[a] Predicted on the basis of superposition of assembly response to individual truss loading.

Failure Modes and Sequence

For each roof, first-truss failure defined roof load capacity. Although they were not coincident events, results indicated that under a gravity-load situation, roof load could not have been increased after the initial failure, which caused a drop in the hydraulic load as a result of a sudden increase in the deflection of one or more trusses. Figure 14 shows the sum of vertical reactions compared to average vertical deflections of the truss peaks during failure testing for each of the three roof assemblies. The load on the assembly at the time of the first failure (marked 1 on Fig. 14) approximates the ultimate load carried by that assembly. Ratios of load at first failure to the ultimate load measured on the assembly are 0.92 for the 3:12 Fink, 1.0 for the 6:12, and 0.99 for the scissors. This analysis suggests that a gravity load, which would not decrease between failures, would likely have led to a cascading sequence of failures beginning with the first failure.

A survey of truss reactions through the sequence of loading to failure indicates that although a few trusses did reach a maximum load prior to the assembly maximum, they continued to provide significant contribution to assembly strength until the roof assembly failed.

Conclusions

This study provides a basis for future developments in the evolution of analytical models and methods to more accurately predict the structural capacity of repetitive member assemblies. Results show that repetitive member roof assemblies behave like parallel systems in which member deflections are controlled by assembly interactions. Thus, they carry load in proportion to their stiffness rather than series systems in which member loads are uniformly distributed, and the weak-link value controls assembly capacity. These results suggest the need to focus on the correlation between stiffness and strength and to develop models to detect strain limits on individual elements and connections in addition to, or in place of, stress limits. Test methods demonstrated the advantages of using superposition to evaluate load distribution and the shortcomings of hydraulic loading systems to simulate assembly failure under gravity loading.

The most significant conclusions from this study are as follows:

1. The load distribution characteristics of a repetitive member assembly under full design load may be characterized without loading any individual truss to its full design load value. When design load is applied along the top chord of an individual truss, 40 to 70 percent of that load is distributed to adjacent trusses by the sheathing, rather than being carried to the reactions of the loaded truss. By measuring all assembly reactions as load is applied to one truss at a time and then superimposing assembly reactions measured for each truss load, the reaction response characteristics of the assembly under full assembly load may be determined. This approach to assembly testing reduces the possibility of truss damage as a result of excessive loading.

2. Two assembly interaction mechanisms contribute to the improved reliability of trusses used in a repetitive member assembly- composite action and load sharing. Composite action between the sheathing and the top chord of a truss serves to increase the effective stiffness by increasing the effective moment of inertia of the chord. For the roof assemblies, the stiffness increase attributed to composite action was 24 percent for the Fink and 7 percent for the scissors. Tests indicated, however, that as load approached the capacity of the assembly, joint slip caused a reduction in the composite action to the point that it did not contribute to a strength increase.

3. The first failure defined assembly failure mode. Assembly interaction that restricts differential deflection between trusses causes loads to be redistributed around areas of local weakness when the entire assembly is loaded. Therefore, when the first truss fails, redistributed loads that concentrate in the area of the first truss failure cause an immediate overload in the same area of adjacent trusses. In this study, although each assembly exhibited a unique failure mode, the majority of the failures within an assembly were the same.

4. The evaluation of interaction effects on strength suggests ratios of measured assembly strength to minimum truss strength that range from 1.09 to 1.47, depending upon truss configuration and assumptions made on the strength of the weakest member. These ratios for ultimate strength indicate that the 15 percent currently applied only to bending stress of individual elements could be applied to the entire truss, contingent on truss type and assembly configuration. Sensitivity analyses conducted using computer models may be able to give a range of assembly increase factors, depending on assembly configuration variables such as truss span, spacing, relative stiffness of the sheathing when compared to the trusses, sheathing to frame connections, and truss boundary conditions.

Acknowledgments

The success of this study was strongly dependent upon the work and dedication of the Forest Products Laboratory, Engineering Mechanics Laboratory, staff. We give special recognition to Roy Traver for his leadership in the construction and testing phases, Mike Grambsch for instrumentation, and Gary Larson for data collection software development.

Funding for this study was provided in part by the wood industry and the U.S. Department of Agriculture. The Truss Plate Institute took a lead role in coordinating support from the industry. Half the funding was supplied through USDA Competitive Grant No. 86-FSTY-9-0180.

This study was conducted as part of a collaborative research agreement between the USDA Forest Service, Forest Products Laboratory, and Forintek Canada Corp. of Vancouver, B.C. The purpose of this cooperative effort was to provide the technical basis and analytical tools to create a light-frame roof assembly design standard to be used with load resistance factor design procedures that are being developed in Canada and the United States.

The results listed in the Part I report of this research program have been used in the development (Cramer and Wolfe 1989), verification (Varoglu 1985), and calibration (Varoglu 1986; Lam and Varoglu 1988) of existing analytical models that analyze light-frame roof assemblies.

Literature Cited

ASTM.1981a. Standard method for establishing structural grades and related allowable properties for visually graded material. D 245–81. American Society for Testing and Materials, Philadelphia, PA.

ASTM.1981b. Standard method for testing plywood in flexure. D 3043–76. American Society for Testing and Materials, Philadelphia, PA.

Boller, K.H.1972. A facility to evaluate three-dimensional performance of house modules. FPL–RN–0225. Madison, WI: U.S. Department of Agriculture, Forest Service, Forest Products Laboratory.

CSA.1980. Methods of test for evaluation of truss plates used in lumber joints. CSA Standard S347–M1980. Canadian Standards Association.

Cramer, S.M.; Wolfe, R.W.1989. A load distribution model for light-frame wood roof assemblies. ASCE Journal of Structural Engineering. 115(10): 2603–2616.

Foschi, R.O.1977. Analysis of wood diaphragms and trusses, Part II. Truss plate connections. Canadian Journal of Civil Engineering. 4(3): 353–362. National Research Council of Canada, Ottawa, Ontario, Can.

Lam, F.; Varoglu, E.1988. Reliability of trusses and roof systems. Western Forest Products Laboratory, Vancouver, BC. Prepared for the Canadian Forestry Service.

NFPA.1988. National design specification for wood construction. National Forest Products Association, Washington, DC.

TPI.1985. Design specification for metal plate connected wood trusses.Truss Plate Institute, Madison, WI.

TPI.1988. Quality standard for metal plate connected wood trusses, QST–88. Truss Plate Institute, Madison, WI.

Varoglu, E.1985. Structural analysis of trusses and roof truss systems. Western Forest Products Laboratory, Vancouver, BC. Prepared for the Canadian Forestry Service.

Varoglu, E.1986. Reliability of trusses and roof systems. Western Forest Products Laboratory, Vancouver, BC. Prepared for the Canadian Forestry Service.

Wolfe, R.W.; McCarthy, M.1989. Structural performance of light-frame roof assemblies—I. Truss assemblies with high stiffness variability. FPL–RP–492. Madison, WI: U.S. Department of Agriculture, Forest Service, Forest Products Laboratory.

Appendix A-Material Properties

Materials used in the roof assembly research program were donated by the wood industry. The American Plywood Association (APA) provided the plywood sheathing along with their measurements of physical and mechanical properties. The lumber used to construct the trusses was purchased with money contributed by the Wood Truss Council of America. Moisture content and modulus of elasticity measurements were made at the Forest Products Laboratory (FPL) with the assistance of Don Percival of the Small Homes Council, University of Illinois, Champaign-Urbana, Illinois.

Modulus of elasticity (MOE) values were determined for all lumber and plywood sheathing before they were used in the truss or roof system construction. Values measured for the plywood are shown in Table A-l, and those measured for the lumber are shown in Table A-2.

The plywood used for the roof systems was 15/32-in. CD exterior grade sheathing with an APA span rating of 16/4. Each plywood sheet was identified by a panel number as shown in Figure A-1. These numbers show the placement of the individual sheets in the roof systems.

The lumber used to construct the trusses was purchased as No. 2 Dense (N2D) Southern Pine. Of the total 228 pieces of lumber, fewer than 20 had a grade stamp; however, all the lumber appeared to be N2D or better. The average MOE determined was 1.86×10^6 lb/in^2 (1.87×10^6 for the 16-ft pieces and 1.72×10^6 for the 12-ft pieces), which is slightly higher than the National Design Specification published value of 1.6×10^6 lb/in^2. The MOE values shown in Table A-2 were determined using the FPL E-computer. The static MOE was also checked on every tenth 16-ft piece and every fifth 12-ft piece.

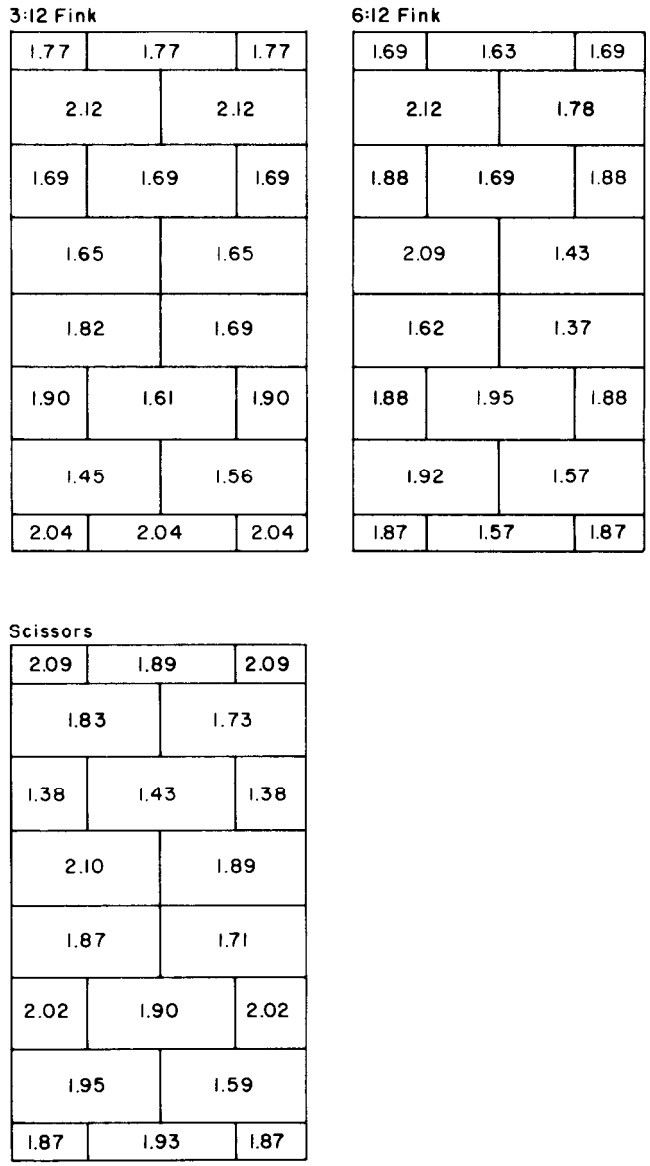

Figure A–1—Roof sheathing layouts and panel stiffness values determined following ASTM D 3043 Method C (1981b). (ML90 5387)

Table A-1–Plywood sheathing modulus of elasticity values[a]

Truss[b]	MOE values ($\times 10^6$ lb/in^2) Top chord North	Top chord South	Bottom chord North	Bottom chord South	Web members[c] NT	NC	ST	SC	Average
T31	2.50	1.62	1.78	2.22	1.85	1.62	1.96	2.03	1.95
T32	2.4	2.2	1.9	2.2	2.1	2.3	2.0	2.2	2.14
T33	1.66	2.13	1.30	1.92	1.68	2.38	1.26	2.53	1.86
T34	2.09	2.55	2.05	1.55	1.85	2.50	2.22	1.26	2.01
T35	1.45	1.31	1.45	1.53	2.56	2.00	2.03	1.98	1.79
T36	1.62	1.88	1.19	1.52	1.68	2.38	1.26	1.50	1.63
T37	1.56	2.20	1.67	1.72	1.62	1.68	2.08	2.03	1.82
T38	2.23	1.84	1.87	1.66	1.72	1.50	1.28	1.28	1.67
T39	2.5	2.4	2.1	2.3	2.3	2.5	2.1	2.4	2.31
T3A	2.05	1.77	1.53	2.84	1.62	2.17	1.98	2.56	2.07
T3B	2.1	2.0	1.8	2.0	1.9	2.1	1.8	2.0	1.97
T3C	2.53	1.78	2.00	1.88	1.72	1.70	1.28	1.85	1.84
T61	1.43	2.45	2.03	1.69	1.96	1.98	2.01	1.79	1.92
T62	1.82	1.52	2.39	1.43	1.58	1.98	2.51	2.08	1.91
T63	1.24	2.18	2.22	1.43	1.90	2.17	1.92	2.01	1.88
T64	1.91	1.38	1.41	1.40	1.82	1.42	1.70	1.50	1.57
T65	1.14	1.85	2.30	2.46	2.12	1.77	1.98	2.73	2.04
T66	2.08	1.84	2.19	1.43	1.86	2.37	1.79	2.17	1.97
T67	1.34	2.39	1.72	2.06	2.07	2.22	1.61	1.98	1.92
T68	1.82	1.77	1.91	1.86	1.96	2.14	1.33	2.28	1.88
T69	2.27	2.08	2.49	1.73	2.26	2.28	1.47	2.59	2.15
T6A	2.01	1.43	2.01	1.47	2.23	2.13	2.18	2.38	1.98
T6B	1.60	1.54	2.06	1.91	2.18	2.21	1.65	1.83	1.87
T6C	2.09	1.49	1.58	1.56	1.21	1.41	1.35	2.00	1.59

[a] Values were measured using 16- and 12-ft lumber prior to being cut for truss fabrication.
[b] MOE values for T32, T39, and T3B were determined by multiplying average values found for corresponding members in other 3:12 trusses by the relative truss stiffness determined in individual truss tests.
[c] NT is north tension web; NC is north compression web; ST is south tension web; SC is south compression web.

Table A-2–Southern Pine lumber modulus of elasticity values

Truss	MOE values ($\times 10^6$ lb/in^2) Top chord North	Top chord South	Web members North 1	South 2	North 3	King post	South 3	South 2	South[a] 1	Bottom chord North	Bottom chord South	Average
TS1	2.55	1.93	1.33	2.37	1.73	2.21	1.93	2.28	—	1.98	2.15	2.05
TS2	1.87	1.51	1.61	1.65	1.73	2.13	1.88	2.28	—	1.52	1.78	1.80
TS3	2.11	1.62	—	1.77	1.39	1.98	1.92	2.37	—	2.61	2.17	1.99
TS4	1.45	1.67	1.35	2.37	1.73	2.28	1.93	2.28	—	1.98	1.98	1.90
TS5	1.88	1.09	2.23	1.65	2.54	2.21	1.88	1.65	—	2.27	2.2	1.96
TS6	2.19	2.63	2.51	1.39	—	2.13	1.88	1.83	—	1.68	1.94	2.02
TS7	2.42	1.81	1.86	2.14	1.52	2.28	2.54	1.42	—	1.71	1.6	1.93
TS8	1.92	1.29	—	1.83	2.37	2.21	1.38	1.77	—	1.34	1.81	1.77
TS9	1.31	1.6	—	2.14	2.37	1.98	1.93	1.77	—	1.69	1.87	1.85
TSA	2.16	1.75	1.92	1.42	1.52	2.13	2.54	1.42	—	2.48	2.01	1.94
TSB	1.58	1.85	2.18	1.83	1.52	2.28	1.38	1.77	—	1.57	2.25	1.82
TSC	1.89	1.7	1.9	2.14	2.37	1.98	1.38	1.77	—	2.33	2.03	1.95

[a] No record of MOE.

Appendix B— Load-Distributing Elements

Loads were distributed away from limber or damaged trusses in the roof assemblies through two major pathways: the bearing plate and the plywood sheathing. The bearing plate contribution is a function of the truss attachment and the tendency for the truss to spread laterally when loaded. The sheathing contribution is a function of relative stiffness of the sheathing and truss and rigidity of the sheathing connection. This appendix is a brief synopsis of the displacement measurements that were taken to give some measure of the function of these two assembly components in the overall performance of a roof assembly.

Bearing Plates

Roof assembly bearing plates were pin connected to the reaction walls to provide lateral restraint. The stiffness of these bearing plates in the horizontal plane, about an axis perpendicular to the length and width, averaged 8.3×10^6 lb/in^2 for the Fink roof assemblies and 19.8×10^6 lb/in^2 for the scissors assembly. These plates were vertically supported on load cells that were placed in line with each truss reaction. When the trusses were loaded individually in the assembly, the bearing plate served as a load distribution beam with multiple supports (individual trusses) and one concentrated load. When the assembly was loaded, it was a pinned-end beam with nine concentrated loads.

Figures B-1 to B-3 show how the bearing plate moved under loads applied to individual trusses. The three lines in each figure represent total spread between bearing plates on the west end, at midlength, and on the east end of the roof. As each truss was loaded, these three readings reflected how much of the lateral force was distributed to other trusses. In each case, when the truss on the west end was loaded, a large portion of the horizontal thrust was transferred to the reaction wall through the bearing plate pin support. Measured displacements of the bearing plate under the west-end truss reaction (0.019 in. for the 3:12 assembly, 0.013 in. for the 6:12, and 0.047 in. for the scissors) represent bending of the plate and some movement of the cantilevered bearing plate pin support. In each case, when load was applied to an end truss, a very slight negative (inward) movement was detected for the bearing plate on the opposite end.

Bearing plate spread at midlength was unique for the scissors assembly. For both Fink truss assemblies, the midlength spread went from zero for load applied to an end truss to its maximum value (0.015 in. for the 3:12 and 0.006 in. for the 6:12) for load applied

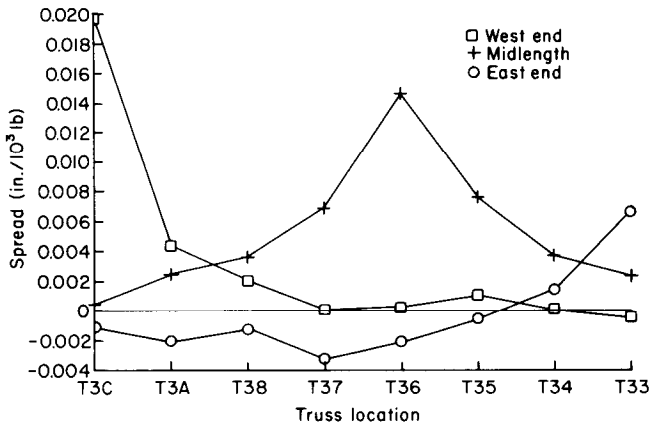

Figure B-1—Depicts the spread measured between bearing plates at three locations along the length of the 3:12 roof as each truss was individually loaded in the assembly. The maximum spread of 0.04 in. was measured for the truss on the west end when it was loaded to 2,200 lb. (ML90 5398)

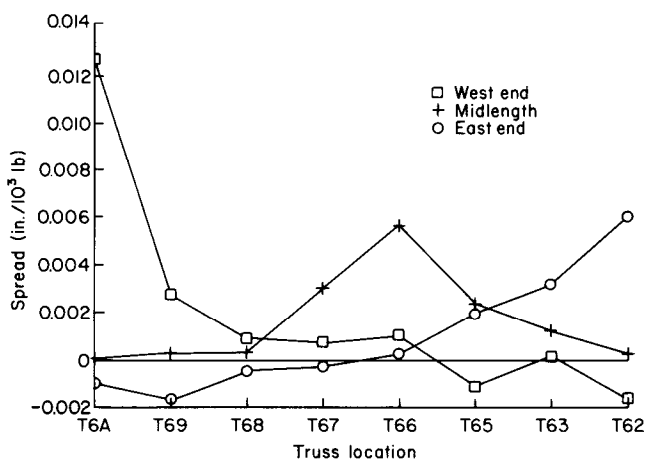

Figure B-2—Depicts the spread measured between bearing plates at three locations along the length of the 6:12 roof as each truss was individually loaded in the assembly. The maximum spread of 0.026 in. was measured for the truss on the west end when it was loaded to 2,800 lb. (ML90 5393)

to the middle truss. For the scissors assembly, the individual trusses provided less resistance to spreading and midlength displacements ranged from 0.008 in. for load on the west-end truss to 0.013 in. for load on the middle truss. When the eighth truss was loaded, a large portion of the horizontal thrust was resisted by the gable end that was a sheathed 6:12 Fink truss.

Table B-1 gives measurements of bearing plate spread under full assembly load. Values given represent the slope of bearing plate spread compared to assembly

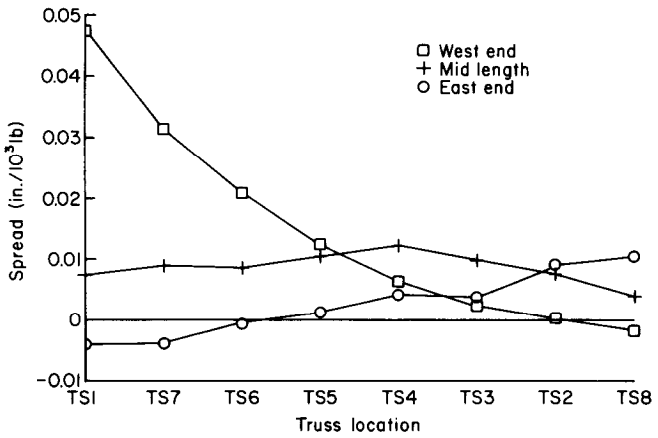

Figure B-3—Depicts the spread measured between bearing plates at three locations along the length of the scissors roof as each truss was individually loaded in the assembly. The maximum spread of 0.095 in. was measured for the truss on the west end when it was loaded to 2,750 lb. (ML90 5388)

Table B-l-Bearing plate separation expressed as a ratio of horizontal displacement to total assembly load

	Separation ($\times 10^{-6}$ in/lb)		
Assembly	West end	Midlength	East end
3:12 Fink	5.50	7.60	1.50
6:12 Fink	2.80	3.00	1.00
Scissors	0.195	0.132	2.30

load. On the west end, the scissors spread was three to six times that of the Fink assemblies.

Plywood Sheathing

To evaluate the importance of the diaphragm action of the sheathing in distribution load among trusses, we placed LVDTs on four trusses and on the gable end in each assembly to monitor movement of the sheathing relative to the truss top chord. In each case, LVDTs were placed at the middle of each top-chord panel and referenced a cantilevered foot that was attached to the sheathing.

Movement of the sheathing with respect to the chord was not unidirectional; therefore, these measurements, oriented parallel to the chord, generated a lot of noise. In many instances, the noise overshadowed our unidirectional measurement.

Sheathing-chord slip measurements support the premise that the sheathing-chord composite action was substantially reduced on critical trusses by the time the maximum assembly load was reached. In general, the largest sheathing movement parallel to the chord occurred on the ends of the roof. For those locations, the sheathing movement with respect to the chord was larger in the panels adjacent to the peak than the panels next to the heels. For interior trusses where we could read the data, displacements were larger close to the heels. The majority of these measurements exceeded 0.015 in. prior to the maximum assembly load. This suggests that the nailed connections were stressed beyond their elastic limit prior to failure of the roof, and thus, composite action should be discounted as a mechanism that increases the strength of a chord-carrying-bending moment. Figures B-4 to B-9 are examples of the load sheathing-chord slip behavior measured for the test assemblies.

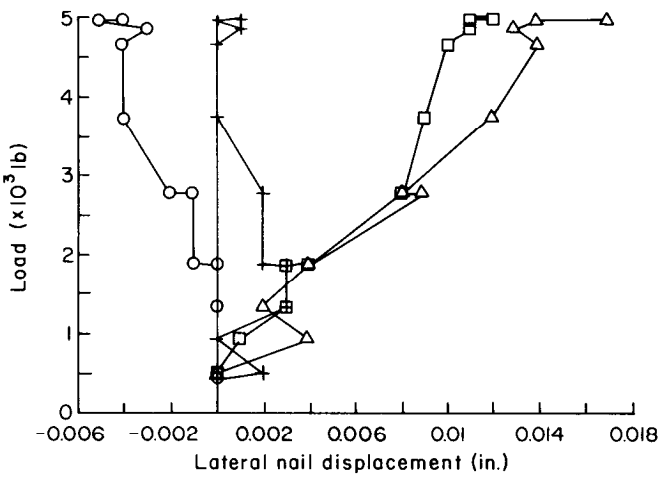

Figure B-l—sheathing-chord slip measurements taken for the seventh truss from the west end of the scissors roof during the full assembly load to failure (ML90 5402)

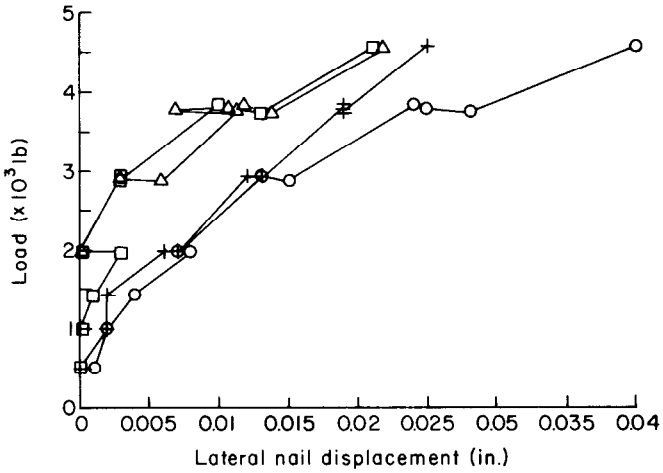

Figure B-5–Sheathing-chord slip measurements taken for the west end truss of the scissors roof during the full assembly load to failure. (ML90 5403)

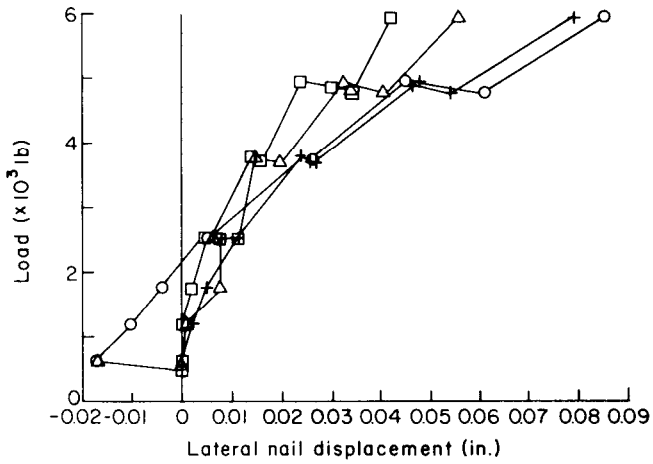

Figure B-6–Sheathing-chord slip measurements taken at the gable end of the 6:12 roof during the full assembly load to failure, (ML90 5394)

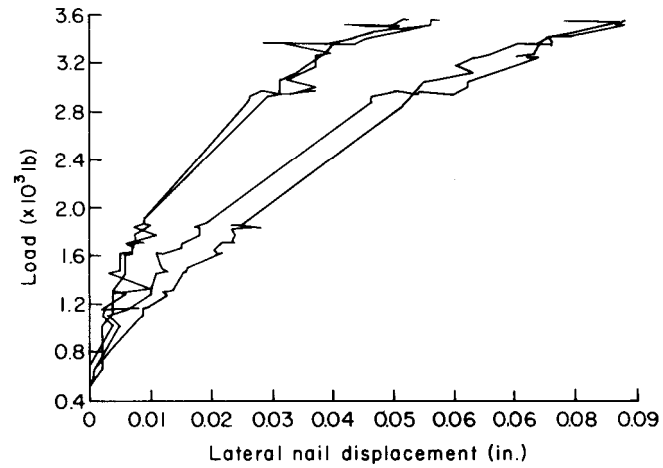

Figure B-7–Sheathing-chord slip measurements taken for the west end truss of the 3:12 roof during the full assembly load to failure. (ML 90 5399)

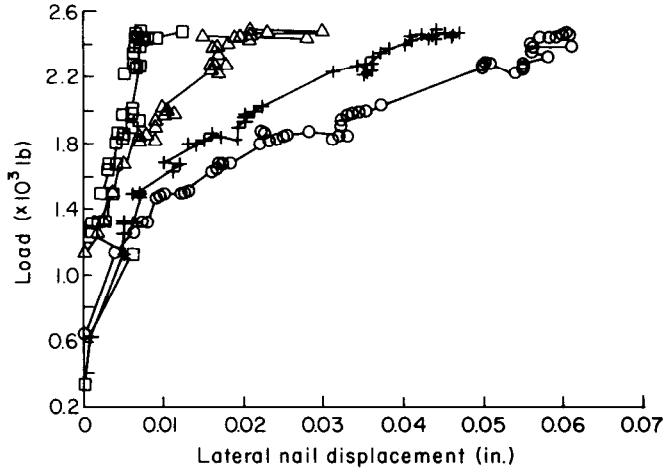

Figure B-8–Sheathing-chord slip measurements taken at the gable end of the scissors during the full assembly load to failure. (ML90 5400)

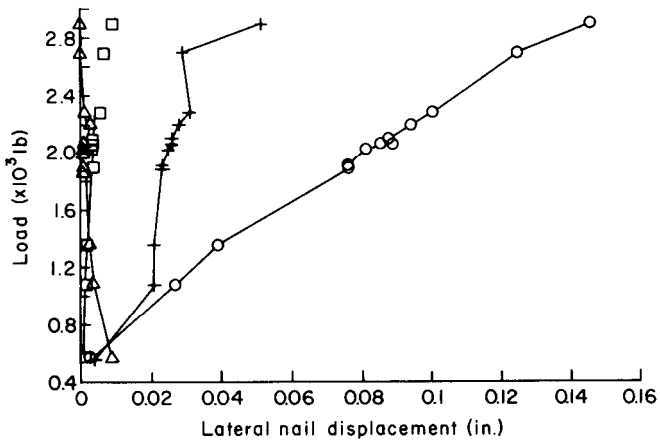

Figure B-g–Sheathing-chord slip measurements taken at the gable end of the 3:12 rosof during the full assembly load to failure. (ML90 5389)

Appendix C—Connections

Points to be considered in modeling truss performance include the characteristic load deformation behavior of metal connector plates (MCPs) and the physical characteristics of the joints. We conducted a series of tests following the CSA S347 standard (CSA 1980) to evaluate the plate-wood interaction behavior for the MCPs used in this study. Prior to testing each truss, we also measured joint gaps and plate misplacement for critical joints.

The CSA standard test was used to derive parameters to fit the following equation, originally proposed by Foschi as a model to estimate the load-slip properties of MCPs.

$$\text{Nail lateral load} = (M_0 + M_1 d) \times [1 - \exp(-Kd/M_0)] \quad (C1)$$

The parameters derived for each of the four basic test orientations are given in Table C-l. These values were derived using the load-displacement curve to maximum load and a least squares nonlinear regression technique. The resulting parameters represent a best fit based on 10 tests at each orientation.

Figure C-1 shows how the joint gap and plate misplacement measurements were taken. Gaps between members at locations A and B shown for each joint (Fig. C-1) were measured with a feeler gauge. Values reported in Tables C-2 to C-4 are the average of measurements on each side of the joints. Plate misplacement was measured using a transparent template that was centered on the joints, as indicated on Figure C-l. Table C-5 gives the maximum and average plate misplacement coordinates for each truss configuration tested. For the Fink heel connections, only a **Y** displacement is given. The plate could be placed over a 2-in. range in the **X** direction without being considered misplaced; therefore, we only measured the distance from the center of the plate from the wood-to-wood joint.

The Truss Plate Institute (TPI) has established a quality standard (QST-88) for metal plate connected wood trusses in which they recommend tolerance limits for plate placement, embedment, and joint gaps (TPI 1988). The TPI recommends that gaps at the truss peak and heel joints be limited to 1/8 in. for the joints surveyed. As for plate placement, the scissors heel plate (3 by 10.5 in.) could be misplaced by up to 1/2 in., and the 3:12 Fink heel plate (3 by 7 in.) could be misplaced by 3/8 in. The limit on all other plates is 1/4 in.

Table C-1–Lateral load resistance of metal plate connectors[a]

Orientation[b]	M_0	M_1	K	Maximum load (lb)
AA	2,400	56,590	1,210,000	3,790
EA	3,080	56,520	1,230,000	4,310
AE	1,375	5,300	509,000	2,430
EE	3,230	-7,250	574,000	2,520

[a] Parameters are fit to the model $(M_0 + M_1 \times d)\ [1 - \exp(-K \times d/M_0)]$.

[b] AA is load applied parallel to the grain and parallel to the principal axis of the plate; EA is perpendicular to grain parallel to principal axis of plate; AE is parallel to grain perpendicular to principal axis of plate; EE is load applied perpendicular to the grain and perpendicular to the principal axis of the plate.

Over 50 percent of the trusses in this study had joint gaps that did not meet the TPI tolerances. For the 3:12 Fink trusses, 4 out of the 12 trusses had gaps exceeding these values. Ten of the 6:12 Fink trusses and 7 of the scissors trusses had gaps exceeding TPI tolerances. Part of this may have been due to changes in moisture content. The 3:12 trusses were measured within a month of fabrication, but the 6:12 Fink and scissors were stored in a dry environment for 3 to 4 months prior to measurement.

Plate misplacement did not appear to be a major problem. All the scissors trusses were within the TPI tolerance. Two 3:12 Fink trusses had heel plates misplaced by more than 0.375 in., and two 6:12 trusses had plate misplacements of more than 0.25 in.

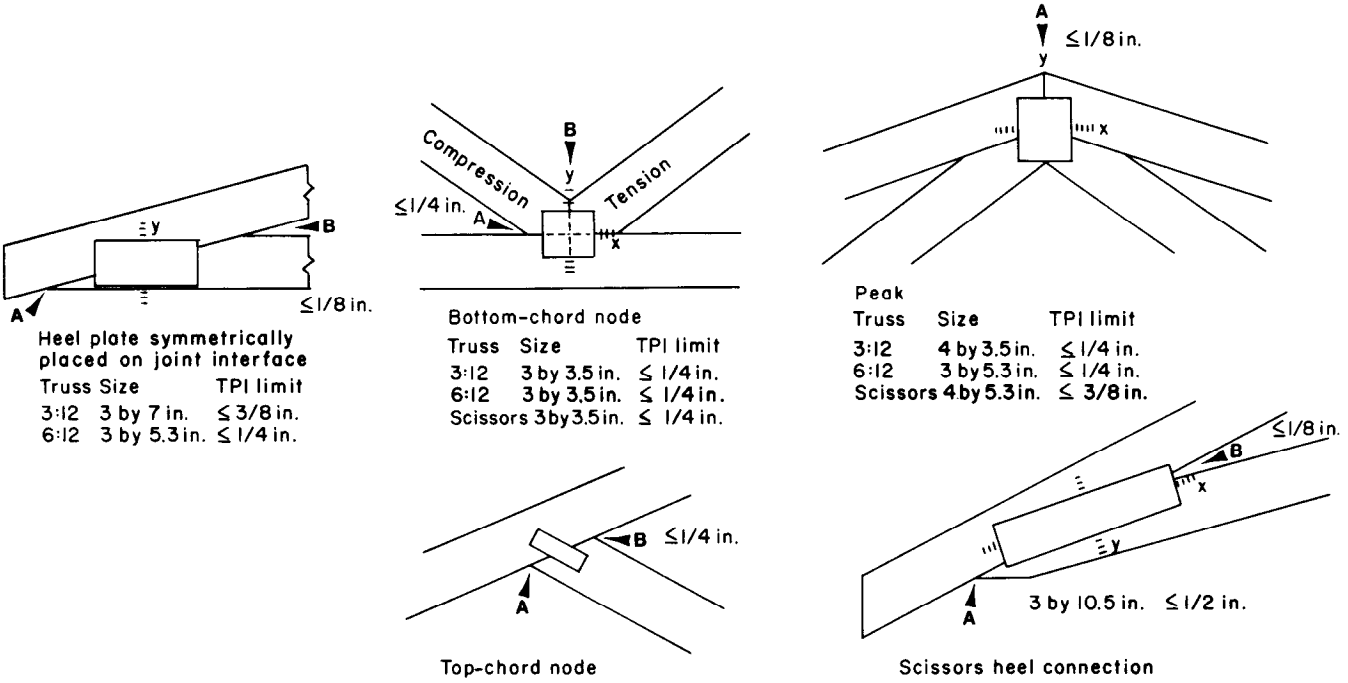

Figure C-1—Plate misplacement and joint gap measurements. Transparent template was placed over the joint. Plate misplacement was read on a scale marked in 0.1-in. increments. (ML90 5384)

Table C-2—Joint gaps for 3:12 trusses measured prior to testing

		Gap measurements (in.)[a]												
		South heel		South top-chord node		South bottom-chord node			North bottom chord node		North top chord node		North heel	
Truss[b]	Side	A	B	A	B	A	B	Peak	B	A	B	A	B	A
T31	East	0.08	0.08	0.10	0.05	0.09	0.08	0.04	0.08	0.03	0.03	0.07	0.07	0.02
	West	0.03	0.05	0.10	0.04	0.04	0.06	0.13	0.02	0.06	0.02	0.06	0.07	0.01
T32	East	0.07	0.05	0.11	0.07	0.07	0.14	0.07	0.07	0.06	0.08	0.06	0.14	0.05
	West	0.07	0.07	0.12	0.07	0.07	0.11	0.02	0.03	0.06	0.06	0.04	0.00	0.05
T33	East	0.03	0.09	0.07	0.02	0.09	0.07	0.09	0.05	0.09	0.07	0.11	0.09	0.09
	West	0.02	0.06	0.06	0.02	0.02	0.03	0.08	0.03	0.06	0.04	0.07	0.07	0.07
T34	East	0.06	0.09	0.12	0.08	0.05	0.09	0.03	0.09	0.03	0.02	0.08	0.10	0.06
	West	0.05	0.06	0.07	0.02	0.03	0.09	0.01	0.06	0.04	0.02	0.06	0.06	0.06
T35	East	0.02	0.04	0.12	0.09	0.04	0.04	0.04	0.10	0.06	0.07	0.09	0.05	0.02
	West	0.03	0.03	0.06	0.03	0.04	0.04	0.04	0.04	0.03	0.03	0.11	0.03	0.02
T36	East	0.01	0.06	0.15	0.08	0.12	0.09	0.04	0.06	0.07	0.06	0.14	0.03	0.02
	West	0.01	0.06	0.08	0.03	0.04	0.06	0.06	0.04	0.07	0.05	0.11	0.03	0.02
T37	East	0.17	0.14	0.11	0.04	0.08	0.03	0.13	0.10	0.06	0.04	0.08	0.11	0.07
	West	0.03	0.04	0.06	0.02	0.03	0.06	0.05	0.02	0.07	0.03	0.08	0.07	0.05
T38	East	0.05	0.09	0.11	0.05	0.07	0.06	0.04	0.07	0.06	0.07	0.15	0.12	0.02
	West	0.11	0.07	0.11	0.05	0.10	0.09	0.06	0.06	0.04	0.04	0.12	0.11	0.02
T39	East	0.12	0.08	0.12	0.06	0.09	0.14	0.02	0.09	0.07	0.07	0.12	0.06	0.16
	West	0.04	0.05	0.09	0.03	0.06	0.09	0.00	0.05	0.07	0.07	0.11	0.11	0.11
T3A	East	0.05	0.16	0.13	0.03	0.09	0.08	0.03	0.07	0.06	0.05	0.10	0.09	0.02
	West	0.04	0.13	0.14	0.02	0.05	0.06	0.02	0.05	0.06	0.04	0.08	0.09	0.10
T3B	East	0.07	0.07	0.13	0.06	0.09	0.07	0.04	0.09	0.05	0.07	0.14	0.08	0.08
	West	0.05	0.05	0.13	0.05	0.09	0.07	0.02	0.08	0.09	0.08	0.14	0.08	0.06
T3C	East	0.05	0.06	0.14	0.08	0.09	0.05	0.07	0.12	0.08	0.05	0.12	0.11	0.04
	West	0.06	0.05	0.09	0.04	0.05	0.07	0.11	0.05	0.07	0.03	0.06	0.09	0.05
Average		0.05	0.07	0.10	0.05	0.07	0.07	0.05	0.06	0.06	0.05	0.09	0.08	0.05
COV[c] (%)		67	45	26	47	40	38	68	42	27	40	32	41	70

[a] Gap measurements:
Heel joints: measurements taken at four corners of top-chord/bottom-chord interface.
Top-chord nodes: measurements at four corners of web/top-chord interface.
Bottom-chord nodes: measurements at compression web/bottom-chord interface and web-web interface.
Peak: measurements at two sides of top-chord/top-chord interface.
Plate misplacement measurements:
Tension web-chord connect: measurements indicate distance from center of joint to centroid of plate.
Heel connections: measurements indicate the vertical distance from plate centroid to joint interface.

[b] Average gap width = 0.09 in.

[c] Coefficient of variation.

Table C-3—Joint gaps for 6:12 trusses measured prior to testing

		Gap measurements (in.)[a]												
		South heel		South top-chord node		South bottom-chord node			North bottom chord node		North top chord node		North heel	
Truss[b]	Side	A	B	A	B	A	B	Peak	B	A	B	A	B	A
T61	East	0.070	0.070	0.090	0.039	0.029	0.090	0.074	0.132	0.070	0.057	0.105	0.110	0.111
	West	0.054	0.066	0.074	0.074	0.020	0.090	0.051	0.057	0.054	0.020	0.054	0.090	0.092
T62	East	0.074	0.057	0.090	0.090	0.090	0.119	0.035	0.104	0.046	0.015	0.042	0.074	0.129
	West	0.054	0.074	0.051	0.051	0.057	0.099	0.053	0.061	0.046	0.042	0.075	0.105	0.129
T63	East	0.085	0.045	0.126	0.091	0.060	0.062	0.126	0.075	0.050	0.020	0.034	0.075	0.107
	West	0.062	0.045	0.058	0.021	0.031	0.045	0.108	0.060	0.039	0.029	0.075	0.021	0.036
T64	East	0.090	0.090	0.088	0.037	0.035	0.074	0.132	0.054	0.031	0.036	0.087	0.039	0.039
	West	0.019	0.064	0.037	0.000	0.010	0.057	0.132	0.037	0.010	0.000	0.043	0.039	0.039
T65	East	0.133	0.133	0.050	0.036	0.090	0.031	0.066	0.121	0.027	0.015	0.058	0.048	0.030
	West	0.110	0.105	0.046	0.036	0.030	0.031	0.066	0.045	0.043	0.029	0.048	0.031	0.030
T66	East	0.085	0.066	0.066	0.056	0.057	0.090	0.000	0.119	0.031	0.020	0.066	0.035	0.097
	West	0.052	0.035	0.056	0.056	0.015	0.074	0.000	0.074	0.165	0.013	0.051	0.165	0.165
T67	East	0.105	0.132	0.074	0.035	0.057	0.070	0.035	0.105	0.031	0.031	0.066	0.124	0.060
	West	0.109	0.057	0.074	0.035	0.039	0.070	0.000	0.074	0.054	0.000	0.029	0.029	0.000
T68	East	0.057	0.057	0.058	0.027	0.045	0.045	0.058	0.018	0.050	0.033	0.075	0.075	0.075
	West	0.054	0.054	0.058	0.027	0.031	0.058	0.058	0.090	0.050	0.010	0.042	0.065	0.086
T69	East	0.132	0.045	0.075	0.060	0.036	0.060	0.119	0.119	0.039	0.033	0.091	0.060	0.075
	West	0.090	0.060	0.033	0.033	0.033	0.075	0.090	0.075	0.020	0.010	0.033	0.060	0.075
T6A	East	0.126	0.108	0.060	0.030	0.050	0.144	0.075	0.147	0.050	0.023	0.060	0.075	0.054
	West	0.050	0.108	0.060	0.010	0.033	0.132	0.060	0.126	0.075	0.011	0.060	0.075	0.165
T6B	East	0.165	0.020	0.051	0.035	0.080	0.080	0.051	0.093	0.058	0.031	0.079	0.034	0.046
	West	0.057	0.000	0.051	0.035	0.010	0.080	0.029	0.093	0.031	0.000	0.031	0.070	0.108
T6C	East	0.165	0.165	0.070	0.047	0.074	0.074	0.090	0.074	0.020	0.010	0.057	0.057	0.033
	West	0.031	0.031	0.033	0.000	0.016	0.051	0.039	0.046	0.027	0.000	0.039	0.074	0.074
Average		0.08	0.07	0.06	0.04	0.04	0.08	0.06	0.08	0.05	0.02	0.06	0.07	0.08
COV[c] (%)		46	54	32	57	54	37	60	39	62	71	34	49	55

[a] Gap measurements:
Heel joints: measurements taken at four corners of top-chord/bottom-chord interface.
Top-chord nodes: measurements at four corners of web/top-chord interface.
Bottom-chord nodes: measurements at compression web/bottom-chord interface and web-web interface.
Peak: measurements at two sides of topchord/top-chord interface.
Plate misplacement measurements:
Tension web-chord connect: measurements indicate distance from center of joint to centroid of plate.
Heel connections: measurements indicate the vertical distance from plate centroid to joint interface.

[b] Average gap width = 0.075 in.

[c] Coefficient of variation.

Table C-4—Joint gaps for scissors trusses measured prior to testing

Truss	Side	Gap measurements (in.)[a] North heel[b] A	B	Peak	South heel B	A
TS1	East	0.165	0.165	0.057	0.045	0.057
	West	0.165	0.165	0.049	0.051	0.057
TS2	East	0.105	0.132	0.039	0.074	0.047
	West	0.105	0.132	0.015	0.039	0.074
TS3	East	0.105	0.105	0.02	0.074	0.057
	West	0.105	0.165	0.02	0.057	0.057
TS4	East	0.165	0.165	0.039	0.165	0.122
	West	0.165	0.155	0.039	0.039	0.039
TS5	East	0.074	0.09	0.064	0.064	0.09
	West	0.074	0.085	0.064	0.039	0.09
TS6	East	0.124	0.074	0.039	0.074	0.074
	West	0.124	0.09	0.039	0.074	0.09
TS7	East	0.119	0.165	0.057	0.057	0.074
	West	0.119	0.165	0.033	0.057	0.057
TS8	East	0.132	0.119	0.132	0.07	0.07
	West	0.132	0.119	0.105	0.07	0.07
TS9	East	0.105	0.044	0.09	0.09	0.09
	West	0.105	0.025	0.039	0.074	0.09
TSA	East	0.119	0.119	0.119	0.057	0.074
	West	0.119	0.119	0.039	0.039	0.074
TSB	East	0.090	0.155	0.132	0.039	0.074
	West	0.090	0.105	0	0.039	0.074
TSC	East	0.057	0.066	0.119	0.074	0.090
	West	0.057	0.039	0	0.015	0.090
Average		0.113	0.115	0.056	0.062	0.074
COV[c] (%)		27	37	69	45	24

[a] Gap measurements: Heel joints: measurements taken at four corners of topchord/bottom-chord interface. Top-chord peak: measurements taken at top of top-chord interface.
[b] A reading of 0.165 signifies a gap ± 0.165 in.
[c] Coefficient of variation.

Table C-5—Plate misplacement measurements[a]

Truss	Plate misplacement (in.)[b] South heel	South bottom-chord node X	Y	Peak X	Y	North bottom-chord node X	Y	North heel	South heel X	Y	Bottom-chord peak X	Y	North heel X	Y
3:12 Fink														
Maximum	0.3	0.4	0.2	0.25	0.2	0.4	0.25	0.3						
Average	0.11	0.9	0.05	0.03	0.08	0.05	0.07	0.09						
6:12 Fink														
Maximum	0.50	0.20	0.15	0.15	0.50	0.20	0.20	0.60						
Average	0.21	-0.02	-0.00	-0.03	0.00	-0.02	-0.02	0.19						
Scissors														
Maximum									0.20	0.10	0.30	0.20	0.50	0.20
Average									-0.03	-0.04	-0.03	-0.07	-0.02	-0.04

[a] Values of X and Y correspond to the coordinates of the centroid of the plate to the centroid of the recommended placement area.
[b] Tension web-chord connections: measurements indicate distance from center of joint to centroid of plate. Heel connections: measurements indicate the distance from plate centroid to joint interface.

Appendix D-Load-Sharing Evaluation

Truss stiffness and strength values given in the Part I report by Wolfe and McCarthy (1989) are listed in Tables D-1 and D-2. Trusses used in that study were designed to have a stiffness variability larger than expected from conventional construction. Critical connections were made using a steel gauge heavier than normally used to decrease the probability of connection failure as a result of steel yielding. Although constructed without gable ends, the roofs in that study did have relatively stiff trusses placed on the ends that were not loaded directly for the assembly load to failure.

Table D-3 gives the Load Sharing Increase Factor (LSIF) values for the Wolfe and McCarthy (1989) roof assemblies, using the same methods that were used to derive LSIF values reported in Table 3. The strong connections and high stiffness variability resulted in increased average strength and increased strength variability. Although the trusses in the Part I report had lower design values than the corresponding trusses in the Part II report, the average assembly strength and minimum truss strength values were 15 percent greater for the 3:12 assembly and 38 percent greater for the 6:12 assembly. As a result, LSIF values calculated for the Part I report were about the same as those reported in the Part II report.

Table D-l-Stiffness and strength for 3:12 Fink trusses[a]

Truss ID	Slope (lb/in)	Failure load (lb) Single	Failure load (lb) Assembly[b]	Assembly maximum (lb)
3EL1	3,230	4,520		
3L3	3,130	5,000		
3L5	2,940	4,240		
3L7	3,330	5,000		
3M1	4,760	6,540		
3M3	4,350	5,780		
3M5	5,000	6,540		
3M7	4,760	7,320		
3H2	5,560	7,320		
3H4	5,000	8,080		
3H6	5,260	7,320		
3H7	5,560	7,320		
3M2	3,560			2,160
3H1	7,190			4,210
3L2	3,640			4,230
3M6	4,170		5,850	5,850
3H5	6,450		5,630	5,630
3L4	2,990		4,140	4,140
3L6	3,480		4,210	4,210
3M4	3,570		4,380	4,380
3H3	5,410			2,440
Average	4,450	6,260	4,840	4140
COV[c] (%)	28	21	19	28

[a] Truss stiffness estimated as the elastic slope of the load-deflection plot. For each assembly, only the middle seven trusses were loaded in the assembly load-to-failure test. Total assembly load at the time of failure is the sum of all nine truss loads. The assembly load divided by the number of trusses loaded compared to individual truss capacity is the assembly effect.

[b] Failed in the assembly load to failure.

[c] Coefficient of variation.

Table D-2—Stiffness and strength for 6:12 Fink trusses[a]

Truss ID	Slope (lb/in)	Failure load (lb) Single	Failure load (lb) Assembly[b]	Assembly maximum (lb)
6L2	10,000	6,010		
6L3	10,000	6,010		
6L5	10,000	6,470		
6L7	9,090	6,010		
6M1	14,290	10,630		
6M2	14,290	9,240		
6M4	16,670	9,240		
6M7	14,290	9,240		
6H1	16,670	11,090		
6H2	16,670	7,390		
6H6	20,000	8,780		
6H7	16,670	9,240		
6M3[b]	11,350		8,700	3,950
6H3[b]	14,080		10,060	7,720
6L1[b]	6,710		7,560	7,330
6M5	9,900		8,840	8,790
6H4	13,510		9,700	9,430
6L4	7,870		6,320	6,320
6L6	8,200		6,980	6,980
6M6	12,480		7,260	7,260
6H5	16,160			4,770
Average	12,800	8,280	8,180	6,950
COV[c] (%)	29	23	18	24

[a] Truss stiffness estimated as the elastic slope of the load-deflection plot. Assembly load-to-failure test-total assembly load at the time of failure is the sum of all nine truss loads. The assembly load divided by the number of trusses loaded compared to individual truss capacity is the assembly effect.

[b] Trusses tested to failure as a group after the roof was tested to failure.

[c] Coefficient of variation.

Table D-3—The inherent Load Sharing Increase Factor values for two roof assemblies[a]

Truss type	Weakest truss maximum load[b] (lb)	Tributary area load at failure[c] (lb) 1	Tributary area load at failure[c] (lb) 2	Load-sharing increase (percent) 1	Load-sharing increase (percent) 2
	4,140	5,320	4,660	29	13
3:12 Fink	4,140	5,320	4,660	29	2

[a] Wolfe and McCarthy 1989.

[b] Weakest truss maximum load is lowest maximum load measured for any truss of the given configuration.

[c] 1—seven loaded trusses are assumed to carry total applied load.
2–the free-end trusses are assumed to each carry half the tributary area load of the seven loaded trusses.

☆ U. S. GOVERNMENT PRINTING OFFICE:1991/543-045/20007